

Supplementary material part 2: the effect of several parameters and the equation describing TPC

Introduction

We studied the simultaneous evolution of dispersal and the TPC of a population during range shifting for different functions describing the trade-off between thermal breadth ($T_{breadth}$) and maximum performance at the optimal temperature (u_{max}). We tested the sensitivity of our results according to different trade-off functions (including varying fecundity, speed of range shifting, carrying capacity and mutation rate). We first outline the different trade-off functions and subsequently report the main results for cases where the thermal optimum is evolvable or not.

Methods:

As the exact cost of an increase in thermal tolerance is unclear and probably differs between species several trade-off functions were applied (Angilletta et al. 2003)¹. Further, because even a high cost might be “hidden” as reviewed in Kassen (2002)², two of the tested functions included an extra parameter (a) allowing for the relaxation of this trade-off. These latter equations are based on the formula used by Chaianunporn and Hovestadt (2012)³.

$$TP = \frac{1}{T_{breadth}\sqrt{2\pi}} \cdot e^{-\frac{(x-(x_{opt}+x_{adap}))^2}{100 \cdot T_{breadth}}} \quad (1)$$

$$TP = e^{-\frac{(x-(x_{opt}+x_{adap}))^2}{100 \cdot T_{breadth}}} \cdot TP_{max} \cdot e^{-a \cdot T_{breadth}} \quad (2)$$

$$TP = e^{-\frac{(x-(x_{opt}+x_{adap}))^2}{100 \cdot T_{breadth}}} \cdot TP_{max} \cdot (1 - a \cdot T_{breadth}) \quad (3)$$

Here, TP refers to the thermal performance of an individual and TP_{max} to the maximum value of TP . Within the competition phase, competitive strength is directly related to performance capacity and as such the different functions describing the TPCs are used as a measure for the competitive strength of an individual. We assumed that when TP is zero or negative, local conditions are too unsuitable for an individual to reproduce. x refers to an individual’s x-coordinate and x_{opt} to the x-coordinate of the global thermal optimum.

The implications and strength of the performance-thermal breadth trade-off, differ between the equations (see Fig S2.1 and S2.2). Equation (1) is applicable to situations in which the thermal

¹ Angilletta, M. J. 2009. *Thermal Adaptation: A Theoretical and Empirical Synthesis*. Oxford: Oxford University Press.

² Chaianunporn, T. and T. Hovestadt. 2012. Concurrent evolution of random dispersal and habitat niche width in host-parasitoid systems. *Ecological Modelling* 247:241-250.

³ Kassen, R. 2002. The experimental evolution of specialists, generalists, and the maintenance of diversity. *Journal of Evolutionary Biology* 15 (2):173-190.

breadth is broadened with no additional resources available. Then, the surface underneath the fitness function will remain constant and an increase in performance at some temperatures will coincide with a decrease at other temperatures (Angilletta et al. 2003). Therefore, equation (1) represents a Gaussian-based function with constant surface beneath the function. Its maximum performance ability (TP_{max}) is allowed to increase indefinitely with decreasing thermal breadth width (Lynch and Gabriel 1987)⁴. Here, however, we forced $T_{breadth}$ to be larger than 0.00025 (under this value the trade-off no longer holds). This is not the case in equation (2) and (3) where (i) the first part of the formula guarantees a larger niche breadth with increasing value of $T_{breadth}$, (ii) the maximum value of competitive ability is fixed (TP_{max}) and (iii) a third part determines the shape and strength (with increasing a) of the trade-off. When applying equation (2), a was either fixed at 1, 5 or 10 and when applying equation (3), a was either fixed at 1, 3 or 5. TP_{max} is always fixed at 10. Generally, equation (3) will penalize a wide niche breadth most severely of all three equations as thermal performance might become negative, preventing survival of particular genotypes even when competitors are absent. This is why the thermal performance of an individual with $T_{breadth}$ 0.4 is even not visualized when a equals 3 or 5 (Fig S2.2). Instead, for equation (1) and (2) the thermal performance of a particular genotype is always positive, although sometimes infinitely small (approaching zero). However, when relaxing the thermal breadth- competitive strength trade-off ($a=1$) for equation (2) and (3) their strength is weaker compared to equation (1) for which the surface beneath the function is constant.

The mutation size of $T_{breadth}$ is either 0.5 or 0.05, depending on the applied TPC (see overview Table S2.1). Also, the interval from which the value of $T_{breadth}$ is drawn at initialization depends on the applied TPC and the strength of its trade-off (a) (see Table S2.1).

Table S2.1: Overview of the range from which $T_{breadth}$ is sampled at initialization for each type of TPC and the corresponding mutationsize.

x_{adap} evolvable	Thermal Performance Curve	range at initialization	mutationsize
not	(3) $a=1$	0-2	0.5
not	(3) $a=3$	0-0.5	0.05
not	(3) $a=5$	0-0.5	0.05
not	(2) $a=1$	0-6	0.5
not	(2) $a=5$	0-6	0.5
not	(2) $a=10$	0-2	0.5
not	(1)	0-0.5	0.05
yes	(3) $a=1$	0-0.5	0.05
yes	(3) $a=3$	0-0.5	0.05
yes	(3) $a=5$	0-0.5	0.05
yes	(2) $a=1$	0-0.5	0.05
yes	(2) $a=5$	0-0.5	0.05
yes	(2) $a=10$	0-0.5	0.05
yes	(1)	0-0.5	0.05

⁴ Lynch, M. and W. Gabriel. 1987. Environmental Tolerance. *American Naturalist* 129 (2):283-303.

Table S2.2 gives an overview of all parameters used within the model and their values in the main document. Extra tested values as part of the sensitivity analyses are also depicted.

Table S2.2: Overview and definition of all parameters.

Parameter	Description	Value applied in final figures	Extra tested values (Supplementary)
t	The number of generations since the start of the simulation	-	-
x	x-coordinate of an individual	-	-
x_{opt}	x-coordinate of global optimum	-	-
TP	Thermal performance of an individual	-	-
TP_{max}	Only applicable for (2) and (3), the maximal thermal performance	10	-
P_{mort}	Chance of mortality during competition phase	-	-
σ_{disp}	Standard deviation of a Gaussian distribution determining dispersal	evolvable	-
x_{adap}	Distance of local optimum to global optimum along x-axis	Fixed at 0 or evolvable	-
$T_{breadth}$	Width of the thermal breadth	evolvable	-
Mut. rate	The chance of occurrence of a mutation during reproduction	0.001	-
Mut. size	Maximal deviation of a mutation towards the parental genotype	$\sigma_{disp}:0.5, x_{adap}:5, \sigma_{gen}$: see table S1	1 for σ_{gen} and σ_{disp}
N^*	Carrying capacity of one grid cell	50	100
cws	Speed of range shifting	1.3	0.5, 2
λ	Mean number of descendants per individual	3	2 and 5

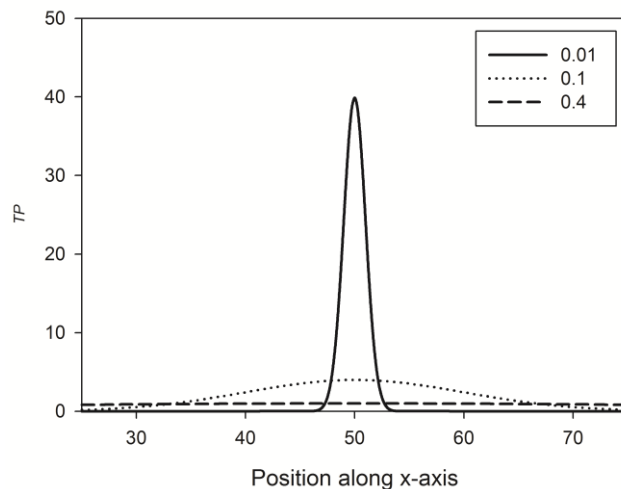


Figure S2.1: Comparison of thermal performance between three different genotypes ($T_{breadth}$) for equation 1. The global optimum is fixed at the 50th column along the x-axis ($x_{opt} = 50$) and local adaptation is not allowed ($x_{adap}=0$). The value of $T_{breadth}$ is indicated in the legend.

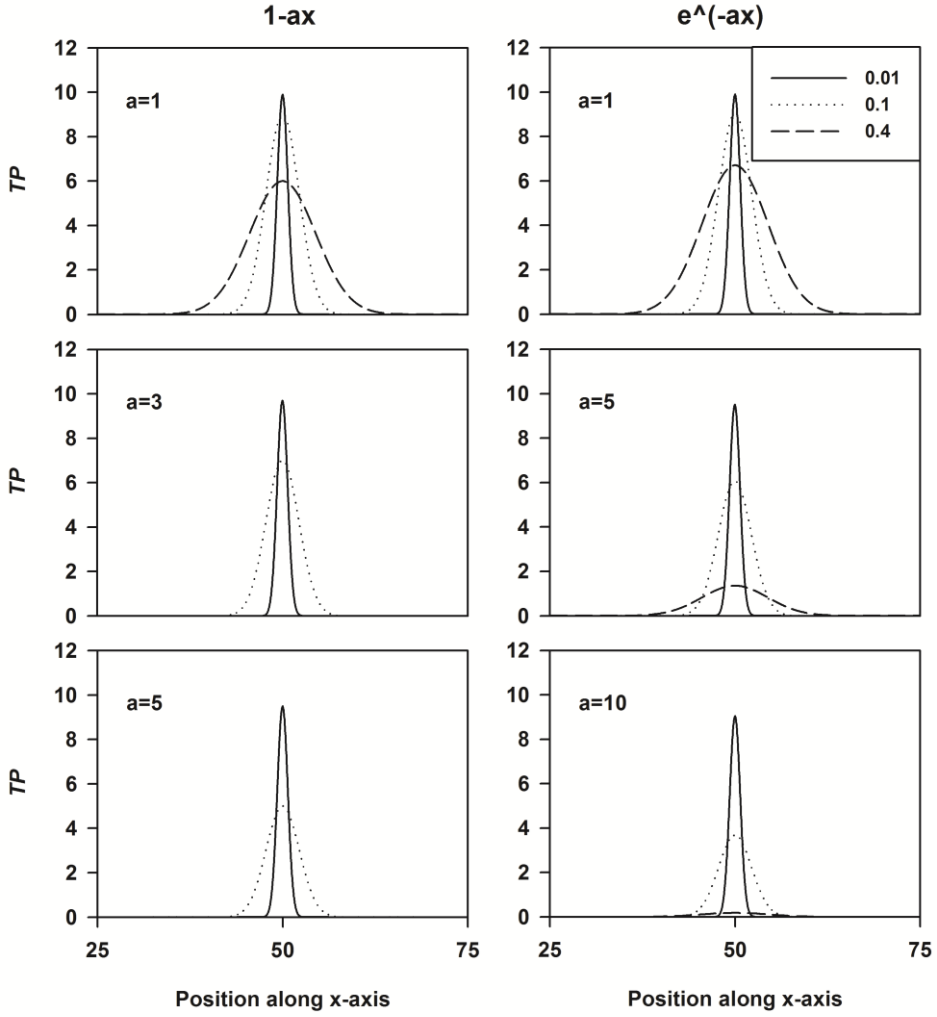


Figure S2.2: Comparison of thermal performance (TP) between three different genotypes ($T_{breadth}$) for equation (2) and (3) for different levels of trade-off strength (a). The global optimum is fixed at the 50th column along the x-axis ($x_{opt}=50$) and local adaptation is not allowed ($x_{adap}=0$). The value of $T_{breadth}$ is indicated in the legend.

Results: evolution of thermal breadth and dispersal in cases where the optimum is not evolvable

When inducing range shifting, the level of dispersal is globally increased within the population. Surprisingly, the least dispersive individuals having the widest thermal breadth dominate at the leading edge. When applying functions (1) or (2) as TPC (Fig S2.4-S2.11; S2.21-S2.26), individuals at the leading edge have the widest thermal breadth of the entire population. Also, when equation (2) is applied, individuals at the front have the lowest dispersive ability of the entire population. For the other equations (1) and (3), the dispersal ability of the individuals at the front is comparable to that of the individuals near the global optimum.

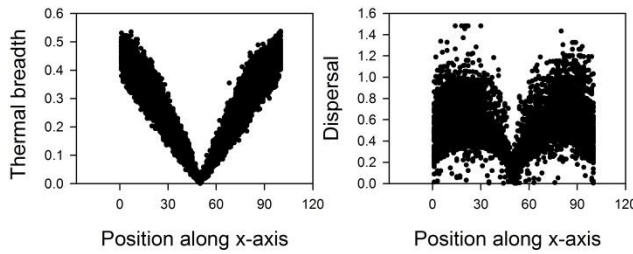


Figure S2.3: The equilibrium in thermal breadth and dispersal before the start of range shifting is displayed in function of position. One dot represents one sampled individual and the global optimum is positioned at the 1349th column along the x-axis. The values of all parameters correspond to those used in the final figures (see Table 1).

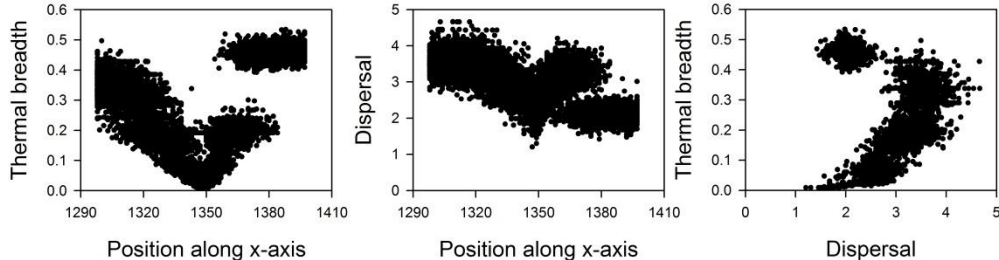


Figure S2.4: The equilibrium in thermal breadth and dispersal during range shifting is displayed in function of position. One dot represents one sampled individual and the global optimum is positioned at the 1349th column along the x-axis. The values of all parameters correspond to those used in the final figures (see Table 1).

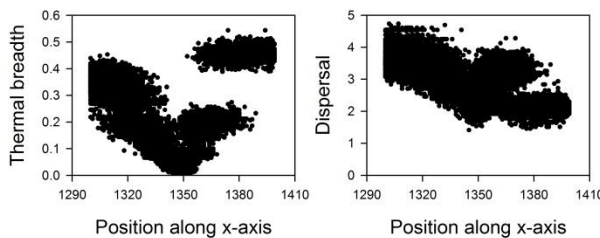


Figure S2.5: The equilibrium in thermal breadth and dispersal during range shifting is displayed in function of position. One dot represents one sampled individual and the global optimum is positioned at the 1349th column along the x-axis. Here, the order of the competition-phase and the displacement-of-global-optimum phase in the lifecycle was switched.

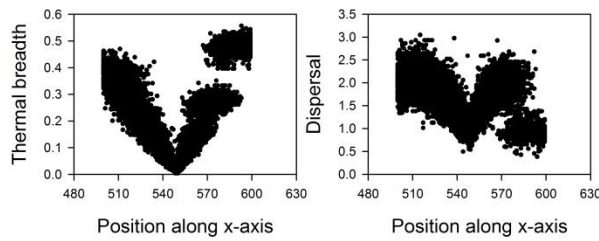


Figure S2.6: The equilibrium in thermal breadth and dispersal during range shifting is displayed in function of position. One dot represents one sampled individual and the global optimum is positioned at the 549th column along the x-axis. The speed of range shifting was decreased to 0.5 columns per generation.

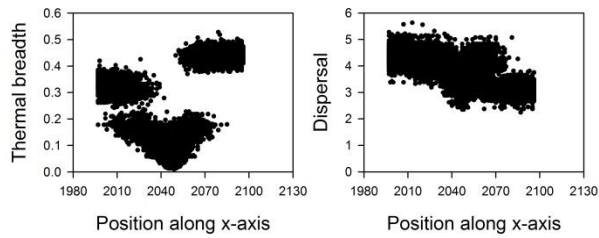


Figure S2.7: The equilibrium in thermal breadth and dispersal during range shifting is displayed in function of position. One dot represents one sampled individual and the global optimum is positioned at the 2049th column along the x-axis. The speed of range shifting was increased to 2 columns per generation. For this scenario, the dimensions of the landscape were increased to 2110 × 100.

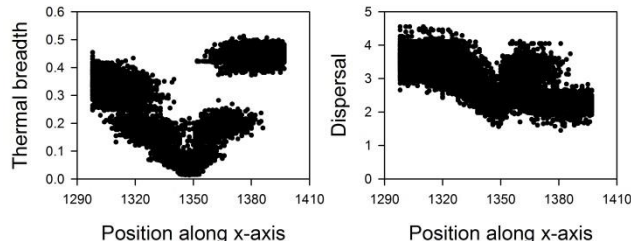


Figure S2.8: The equilibrium in thermal breadth and dispersal during range shifting is displayed in function of position. One dot represents one sampled individual and the global optimum is positioned at the 1349th column along the x-axis. λ was decreased to 2.

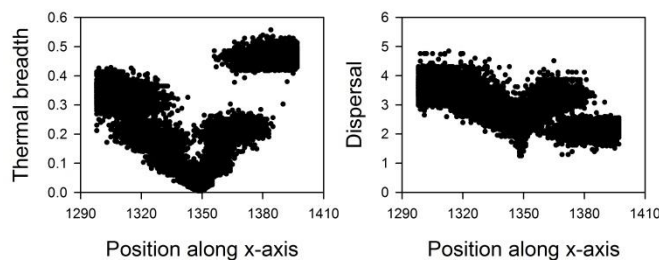


Figure S2.9: The equilibrium in thermal breadth and dispersal during range shifting is displayed in function of position. One dot represents one sampled individual and the global optimum is positioned at the 1349th column along the x-axis. λ was increased to 5.

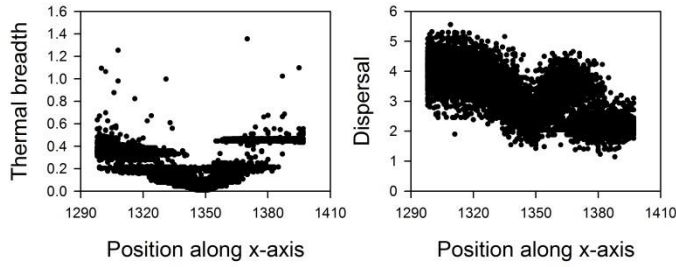


Figure S2.10: The equilibrium in thermal breadth and dispersal during the start of range shifting is displayed in function of position. One dot represents one sampled individual and the global optimum is positioned at the 1349th column along the x-axis. The mutation sizes of both dispersal and thermal breadth were increased to 1.

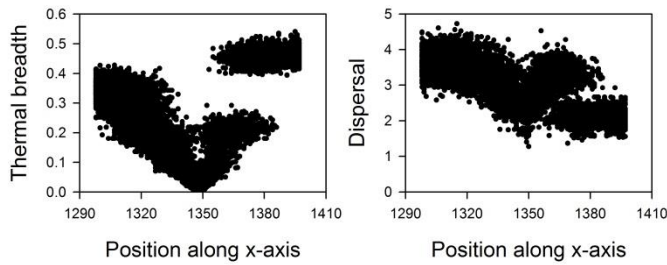


Figure S2.11 The equilibrium in thermal breadth and dispersal during range shifting is displayed in function of position. One dot represents one sampled individual and the global optimum is positioned at the 1349th column along the x-axis. N^* was increased to 100.

When eq. (3) is applied, individuals at the front have a thermal breadth of equal width as the individuals at the trailing edge (Fig S2.12-S2.20). The individuals at the front clearly differ genetically from the rest of the population both in dispersal ability and thermal breadth, being most pronounced for eq. (1) and eq. (2) when the strength of the trade-off is weak ($a=1$) (Fig S2.4-S2.12; S.21-26). In case of eq. (3), the population near the front mainly differs in dispersal ability than in thermal breadth (Fig S2.13). This results in the coexistence of two different genotypes just behind the leading edge. Depending on the applied trade-off function, the area of coexistence lies near the leading edge (Fig S2.21-S2.26) or at a larger distance (Fig S2.4-S2.11; S2.13-S2.20). As within a stationary range, the maximum thermal breadth observed within a population decreases with elevated strength of the performance - thermal breadth trade-off. Only for eq. (2), a simultaneous lowering of dispersal ability is observed within the population (Fig 3- main manuscript).

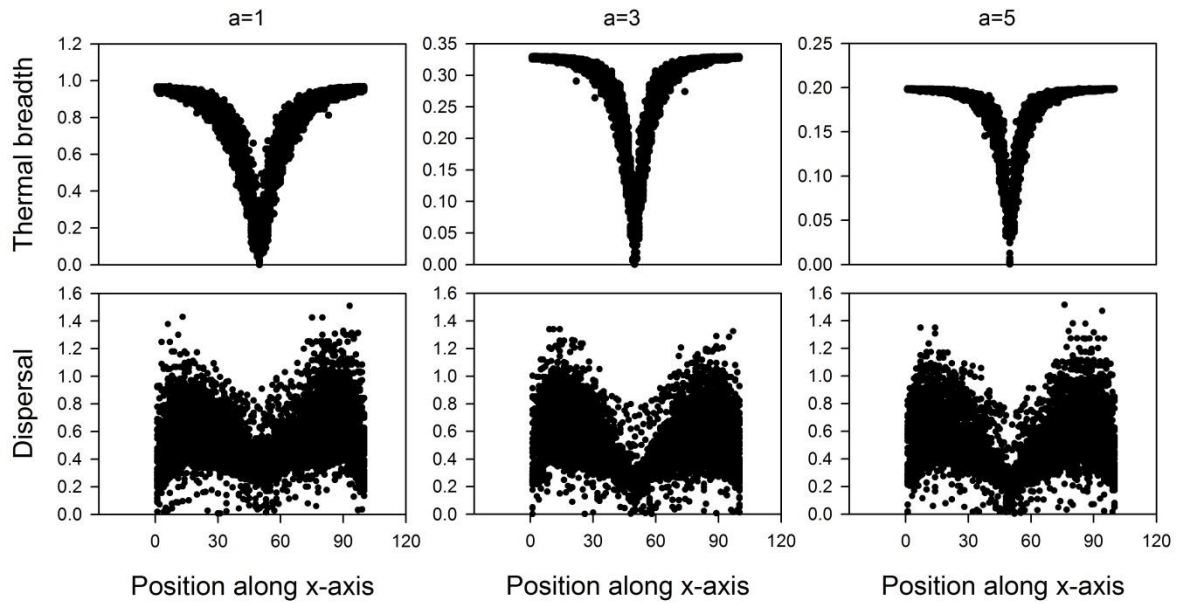


Figure S2.12: For several strengths of the performance-thermal breadth trade-off (equation 3; a equaling 1, 3 or 5), the resulting equilibrium in thermal breadth and dispersal before the start of range shifting is displayed in function of position. One dot represents one sampled individual and the global optimum is positioned at the 1349th column along the x-axis. The values of all parameters correspond to those used in the final figures (see Table 1).

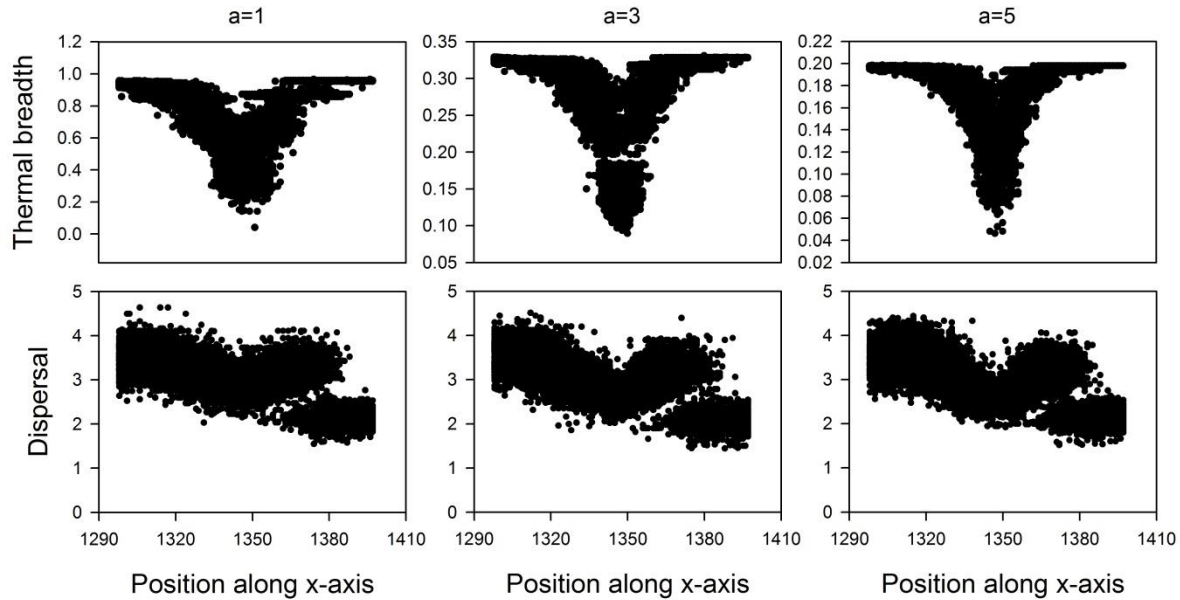


Figure S2.13: For several strengths of the performance-thermal breadth trade-off (equation 3, a equaling 1, 3 or 5), the resulting equilibrium in thermal breadth and dispersal during range shifting is displayed in function of position. One dot represents one sampled individual and the global optimum is positioned at the 1349th column along the x-axis. The values of all parameters correspond to those used in the final figures (see Table 1).

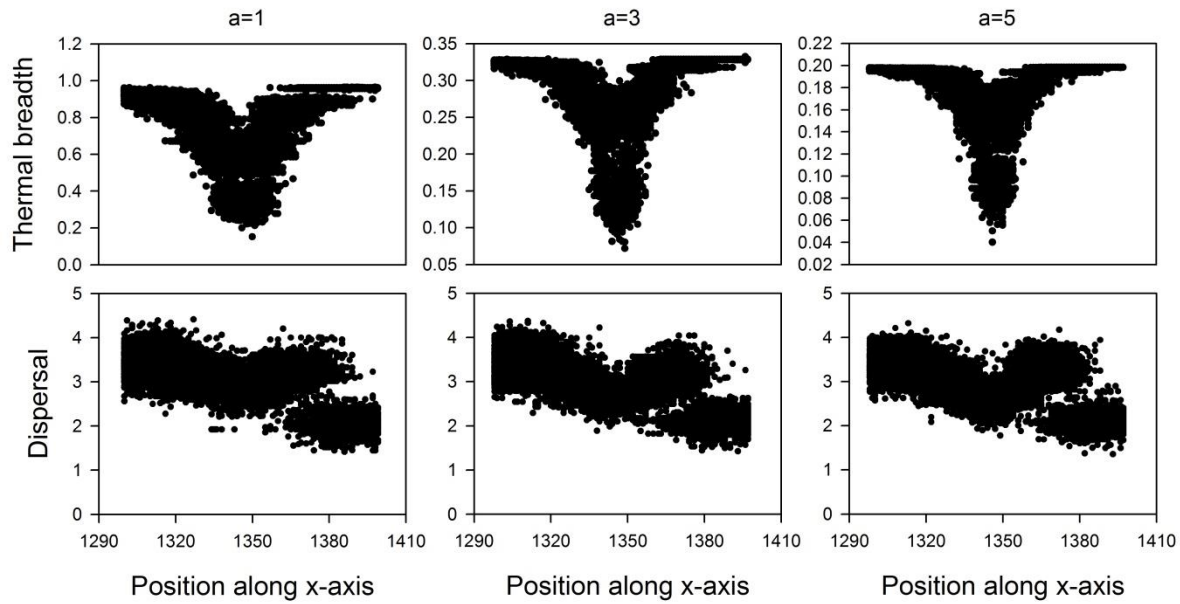


Figure S2.14: For several strengths of the performance-thermal breadth trade-off (equation 3, a equaling 1, 3 or 5), the resulting equilibrium in thermal breadth and dispersal during range shifting is displayed in function of position. One dot represents one sampled individual and the global optimum is positioned at the 1349th column along the x-axis. Here, the order of the competition-phase and the displacement-of-global-optimum phase in the lifecycle was switched.

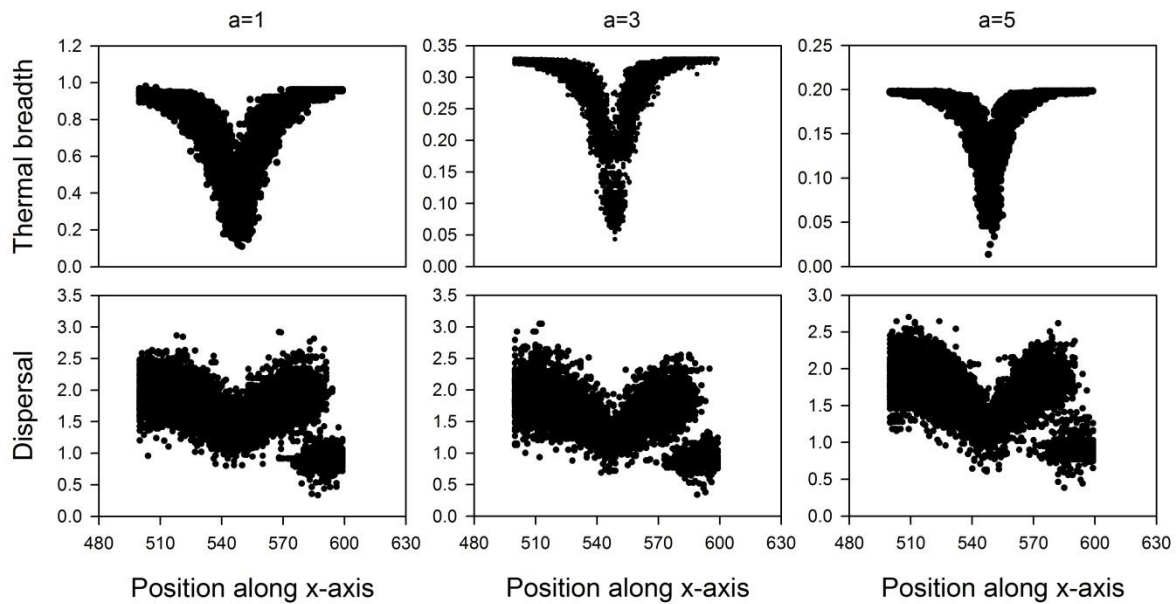


Figure S2.15: For several strengths of the performance-thermal breadth trade-off (equation 3; a equaling 1, 3 or 5), the resulting equilibrium in thermal breadth and dispersal during range shifting is displayed in function of position. One dot represents one sampled individual and the global optimum is positioned at the 549th column along the x-axis. The speed of range shifting was decreased to 0.5 columns per generation.

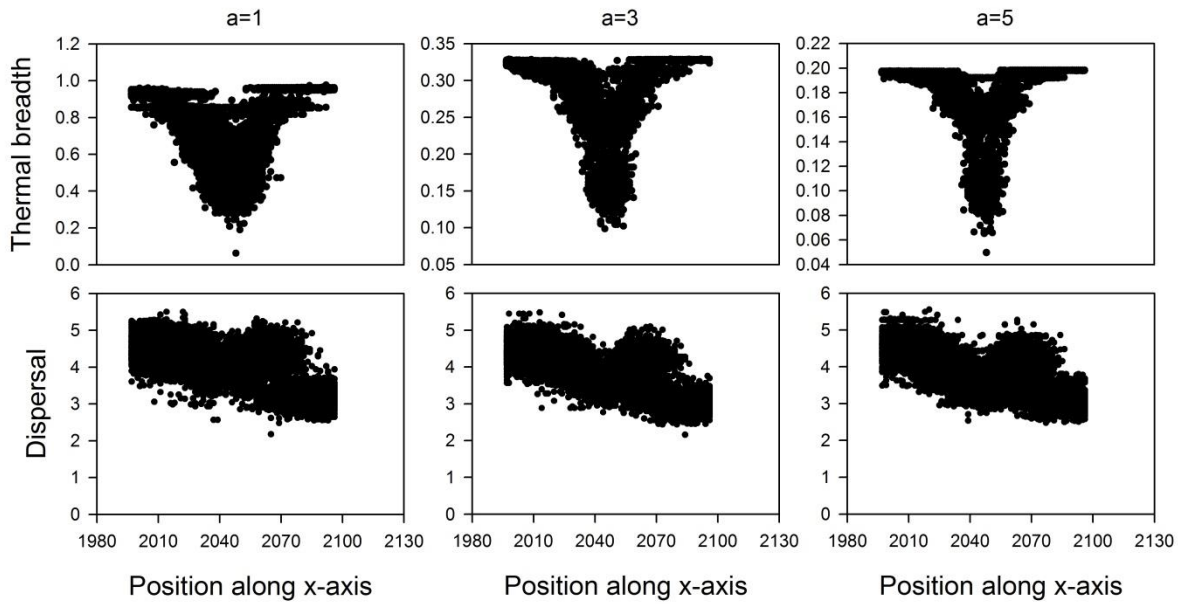


Figure S2.16: For several strengths of the performance-thermal breadth trade-off (equation 3, α equaling 1, 3 or 5), the resulting equilibrium in thermal breadth and dispersal during range shifting is displayed in function of position. One dot represents one sampled individual and the global optimum is positioned at the 2049th column along the x-axis. The speed of range shifting was increased to 2 columns per generation. For this scenario, the dimensions of the landscape were increased to 2110×100 .

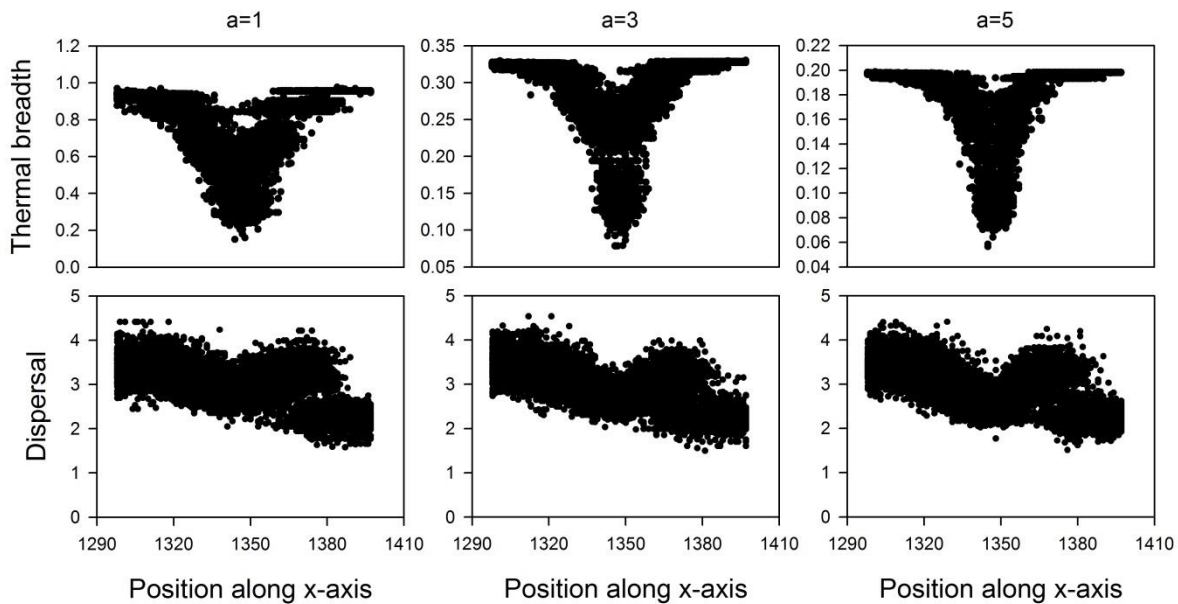


Figure S2.17: For several strengths of the performance-thermal breadth trade-off (equation 3, α equaling 1, 3 or 5), the resulting equilibrium in thermal breadth and dispersal during range shifting is displayed in function of position. One dot represents one sampled individual and the global optimum is positioned at the 1349th column along the x-axis. λ was decreased to 2.

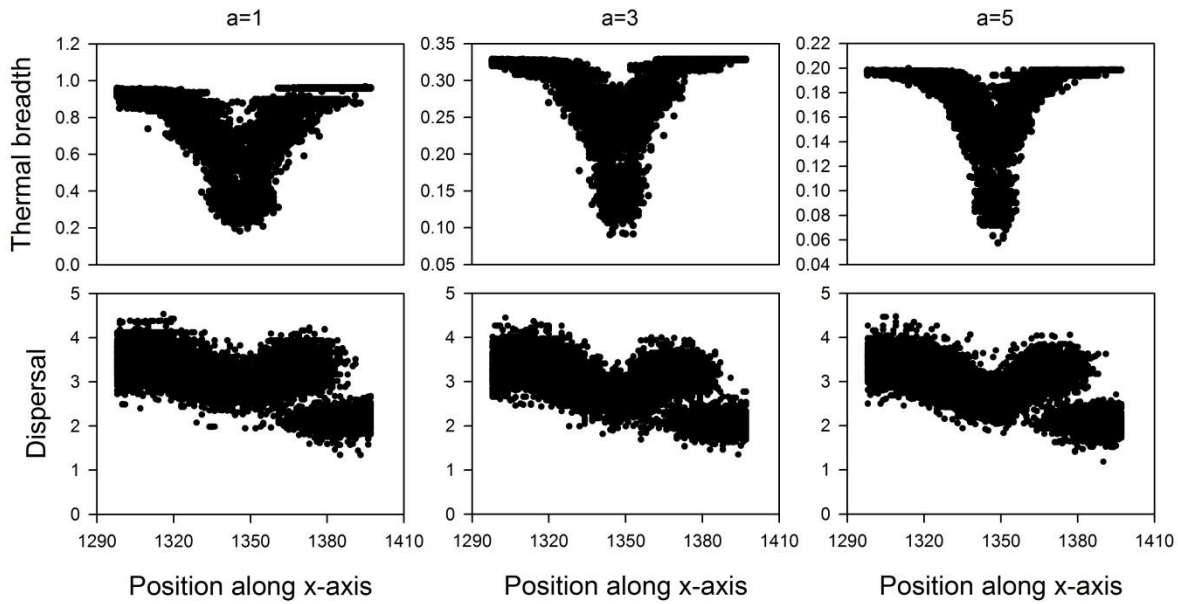


Figure S2.18: For several strengths of the performance-thermal breadth trade-off (equation 3, α equaling 1, 3 or 5), the resulting equilibrium in thermal breadth and dispersal during range shifting is displayed in function of position. One dot represents one sampled individual and the global optimum is positioned at the 1349th column along the x-axis. λ was increased to 5.

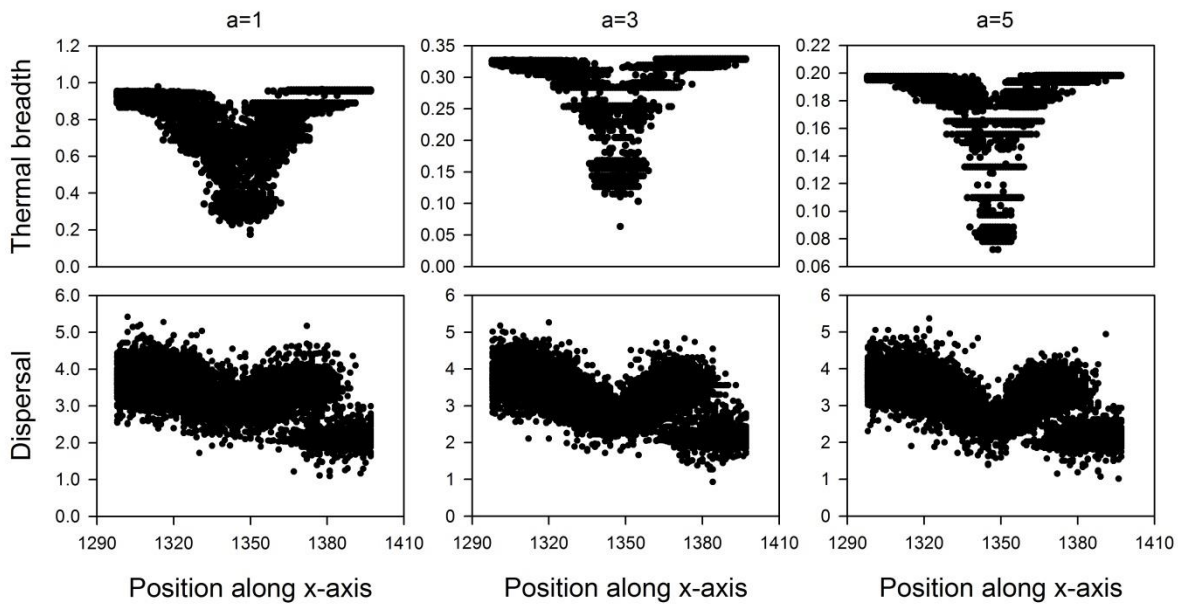


Figure S2.19: For several strengths of the performance-thermal breadth trade-off (equation 3, α equaling 1, 3 or 5), the resulting equilibrium in thermal breadth and dispersal during range shifting is displayed in function of position. One dot represents one sampled individual and the global optimum is positioned at the 1349th column along the x-axis. The mutation sizes of both dispersal and thermal breadth were increased to 1.

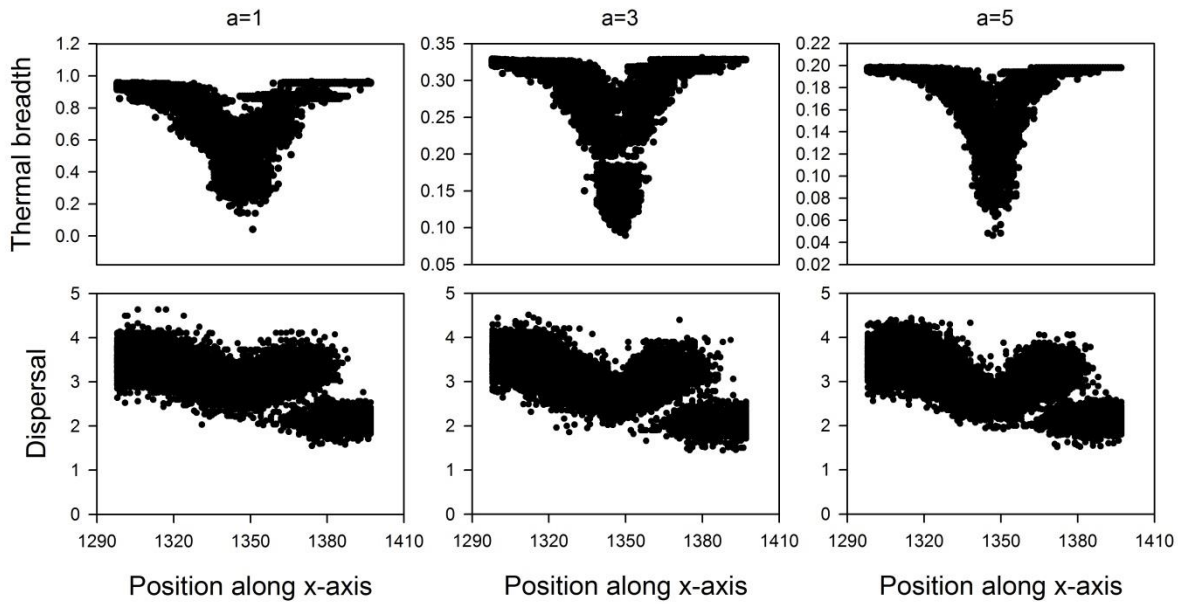


Figure S2.20: For several strengths of the performance-thermal breadth trade-off (equation 3; α equaling 1, 3 or 5), the resulting equilibrium in thermal breadth and dispersal during range shifting is displayed in function of position. One dot represents one sampled individual and the global optimum is positioned at the 1349th column along the x-axis. N^* was increased to 100.

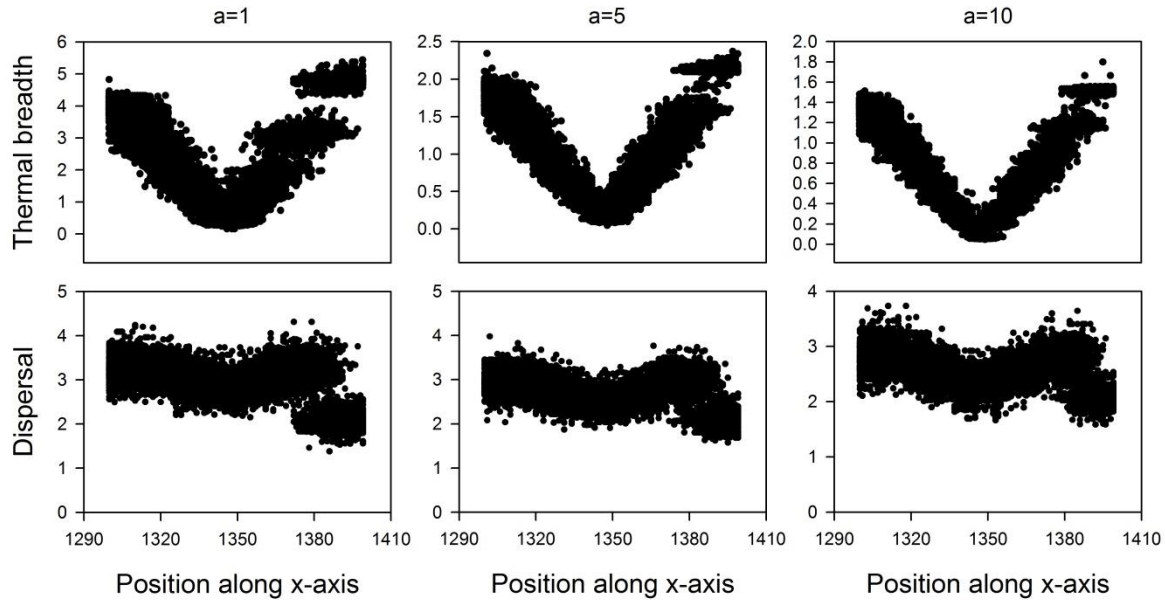


Figure S2.21: For several strengths of the performance-thermal breadth trade-off (equation 2, α equaling 1, 5 or 10), the resulting equilibrium in thermal breadth and dispersal during range shifting is displayed in function of position. One dot represents one sampled individual and the global optimum is positioned at the 1349th column along the x-axis. Here, the order of the competition-phase and the displacement-of-global-optimum phase in the lifecycle was switched.

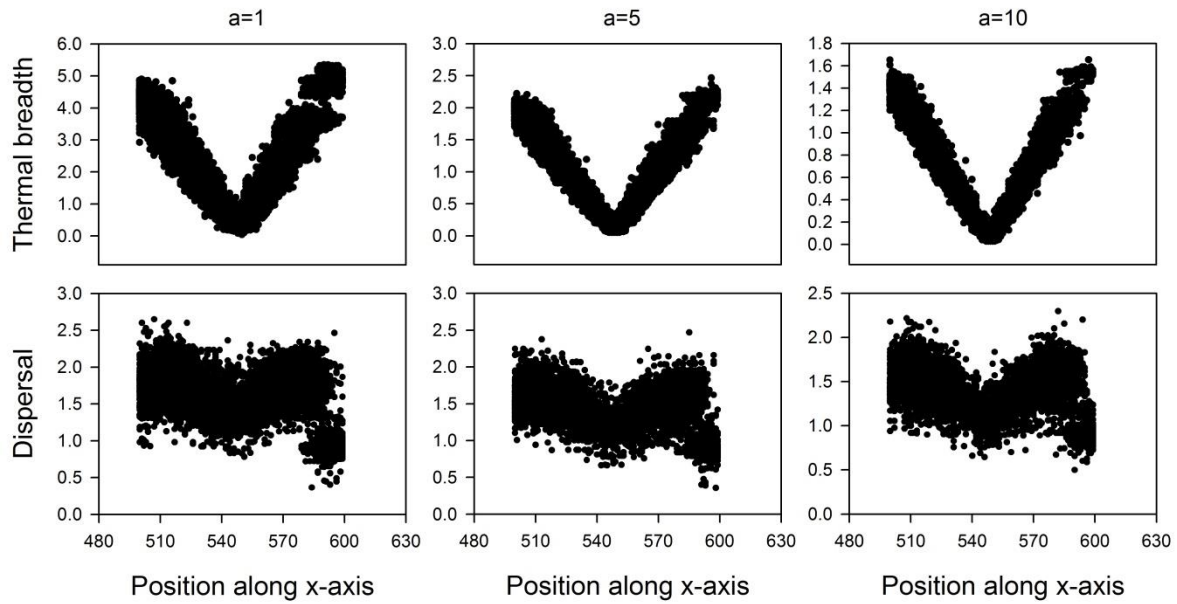


Figure S2.22: For several strengths of the performance-thermal breadth trade-off (equation 2, α equaling 1, 5 or 10), the resulting equilibrium in thermal breadth and dispersal during range shifting is displayed in function of position. One dot represents one sampled individual and the global optimum is positioned at the 549th column along the x-axis. The speed of range shifting was decreased to 0.5 columns per generation.

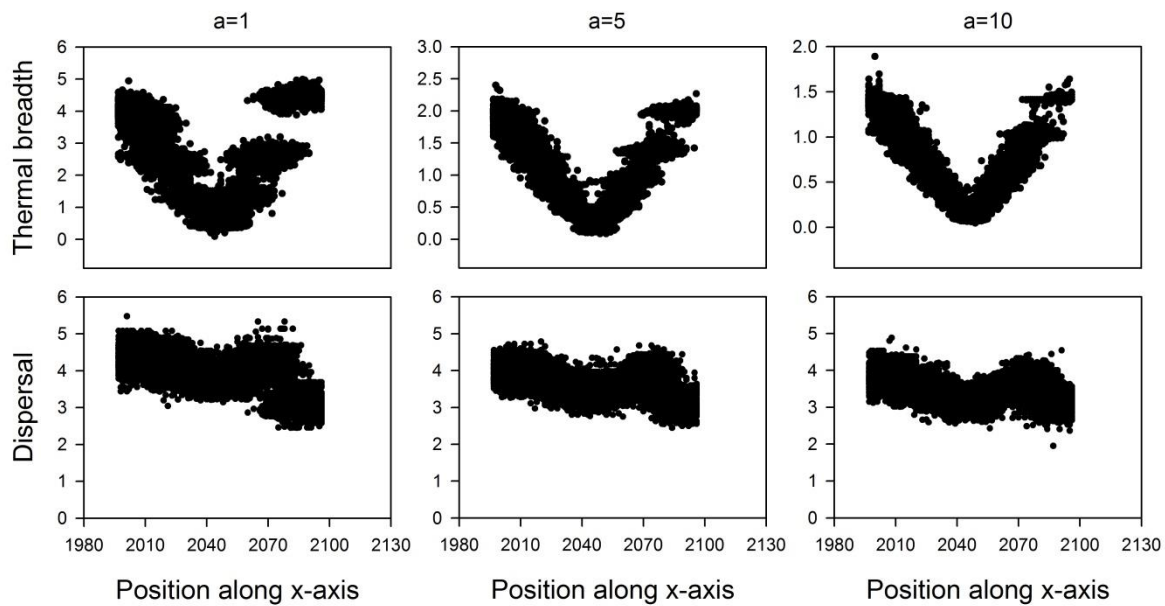


Figure S2.23: For several strengths of the performance-thermal breadth trade-off (equation 2, α equaling 1, 5 or 10), the resulting equilibrium in thermal breadth and dispersal during range shifting is displayed in function of position. One dot represents one sampled individual and the global optimum is positioned at the 2049th column along the x-axis. The speed of range shifting was increased to 2 columns per generation. For this scenario, the dimensions of the landscape were increased to 2110 × 100.

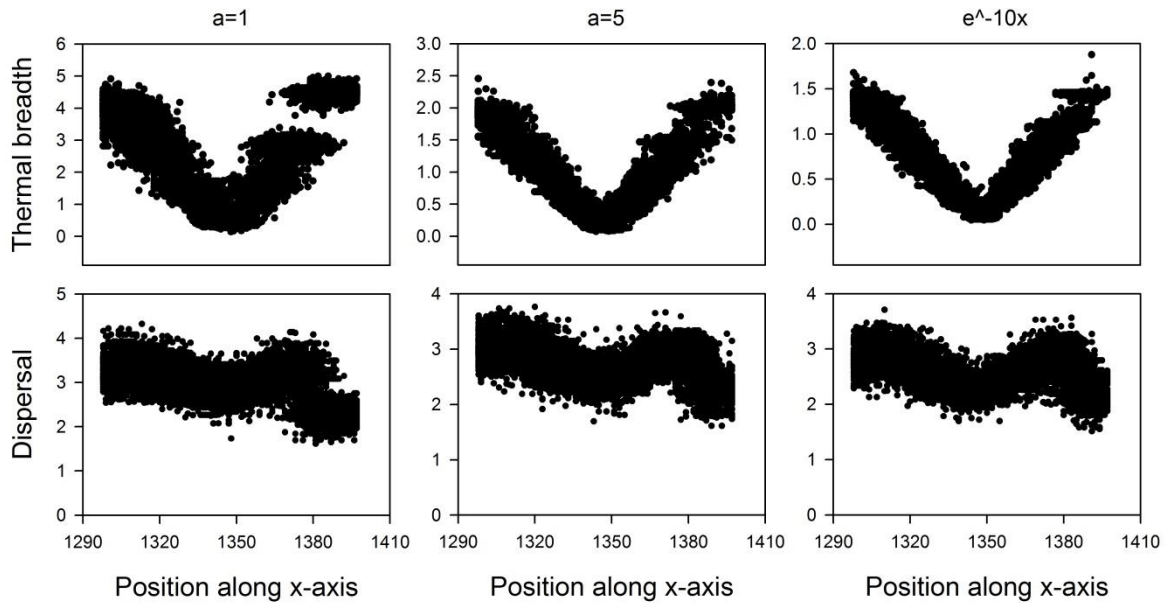


Figure S2.24: For several strengths of the performance-thermal breadth trade-off (equation 2, α equaling 1, 5 or 10), the resulting equilibrium in thermal breadth and dispersal during range shifting is displayed in function of position. One dot represents one sampled individual and the global optimum is positioned at the 1349th column along the x-axis. λ was decreased to 2.

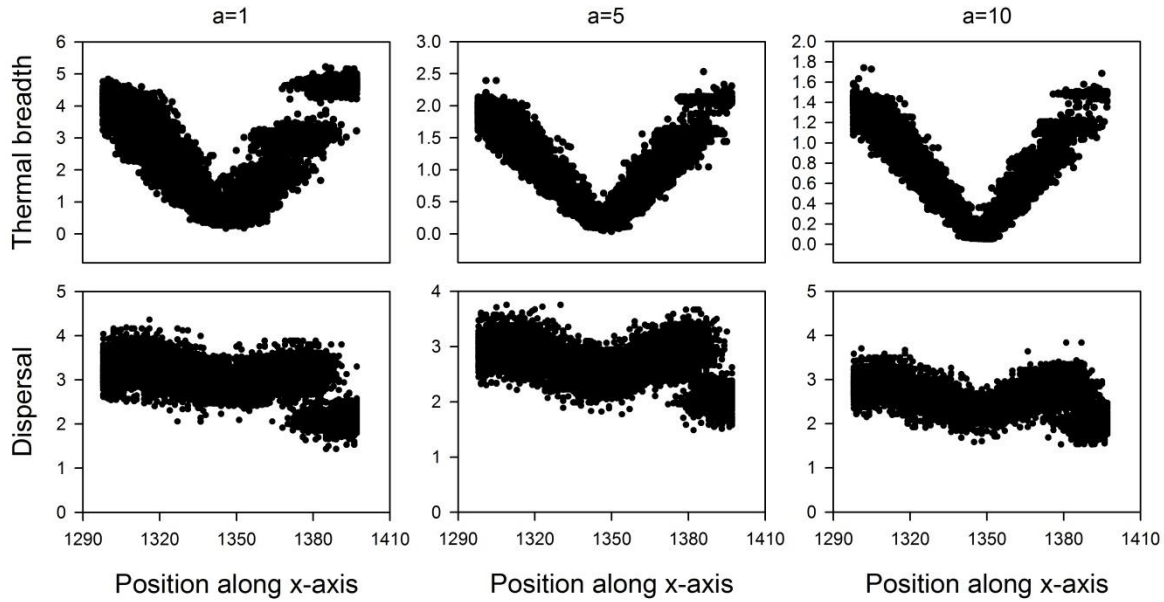


Figure S2.25: For several strengths of the performance-thermal breadth trade-off (equation 3, α equaling 1, 5 or 10), the resulting equilibrium in thermal breadth and dispersal during range shifting is displayed in function of position. One dot represents one sampled individual and the global optimum is positioned at the 1349th column along the x-axis. λ was increased to 5.

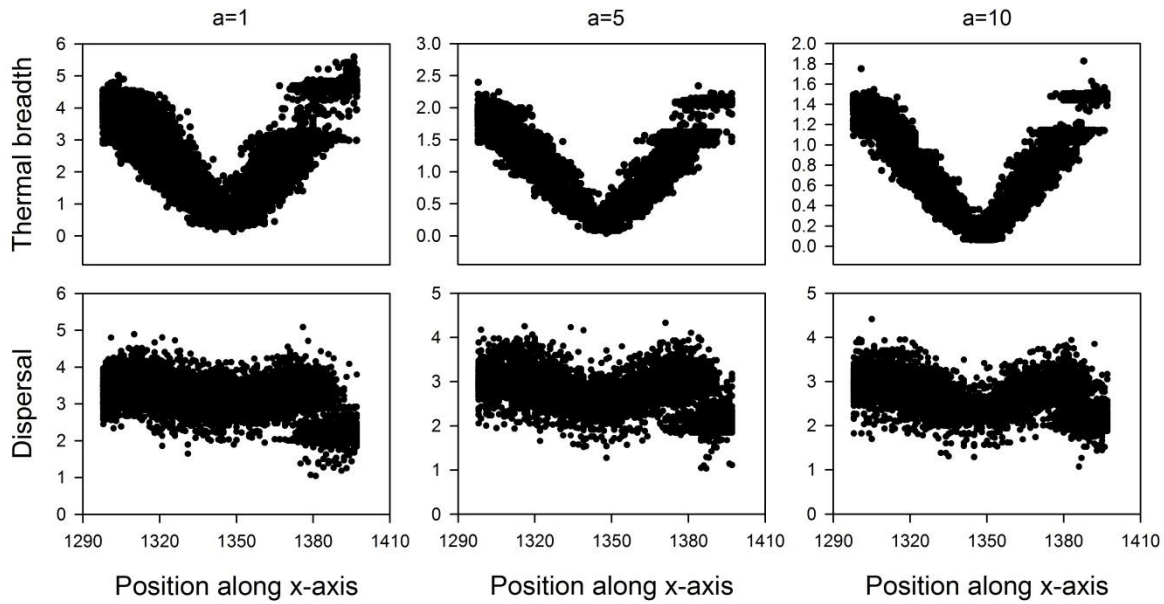


Figure S2.26: For several strengths of the performance-thermal breadth trade-off (equation 3, a equaling 1, 5 or 10), the resulting equilibrium in thermal breadth and dispersal during range shifting is displayed in function of position. One dot represents one sampled individual and the global optimum is positioned at the 1349th column along the x-axis. The mutation size for both dispersal and thermal breadth were increased to 1.

When the speed of range shifting is increased, dispersal within the entire range elevates as well (Fig S2.7; S2.16; S2.23). Further, no qualitative changes of the main results are observed within the sensitivity analyses.

Globally, a strategy occupies a broader range within the range shifting scenario than the static one. This is mainly due to the elevated level of dispersal generating an increased immigration load (GarciaRamos and Kirkpatrick 1997)⁵. Also, this prevents individuals near the trailing edge from encoding the local optimal thermal breadth to persist during range shifting. However, this is only the case when the applied function for the TPC allows for an indefinite increase in thermal breadth towards the range edges (i.e. eq. (1) and eq. (2)) and dispersal is substantially high (i.e. when the trade-off is weak) (Fig S2.4-S2.11; S2.21-S2.26).

⁵ GarciaRamos, G. and M. Kirkpatrick. 1997. Genetic models of adaptation and gene flow in peripheral populations. *Evolution* 51 (1):21-28

Results: evolution of thermal breadth and dispersal in cases where the optimum is evolvable

Before the evolution of range shifting, the thermal breadth and dispersal capacity are overall low within the population. The mean level of thermal breadth decreases with increasing strength of the performance-thermal breadth trade-off. An individual's local thermal optimum coincides almost completely with its own location (Fig S2.27). As expected, this relationship is more accurate with increasing strength of the performance-thermal breadth trade-off (Fig S2.27). When range shifting is induced, both the mean thermal breadth and dispersal capacity increase within the population. However, when the strength of the performance-thermal breadth trade-off is weak, individuals at the leading edge have a narrower thermal breadth than the rest of the population. When the strength of this trade-off is stronger, both traits are uniformly distributed within the range. This is also true when eq. (3) is applied (Fig S2.28-S2.43).

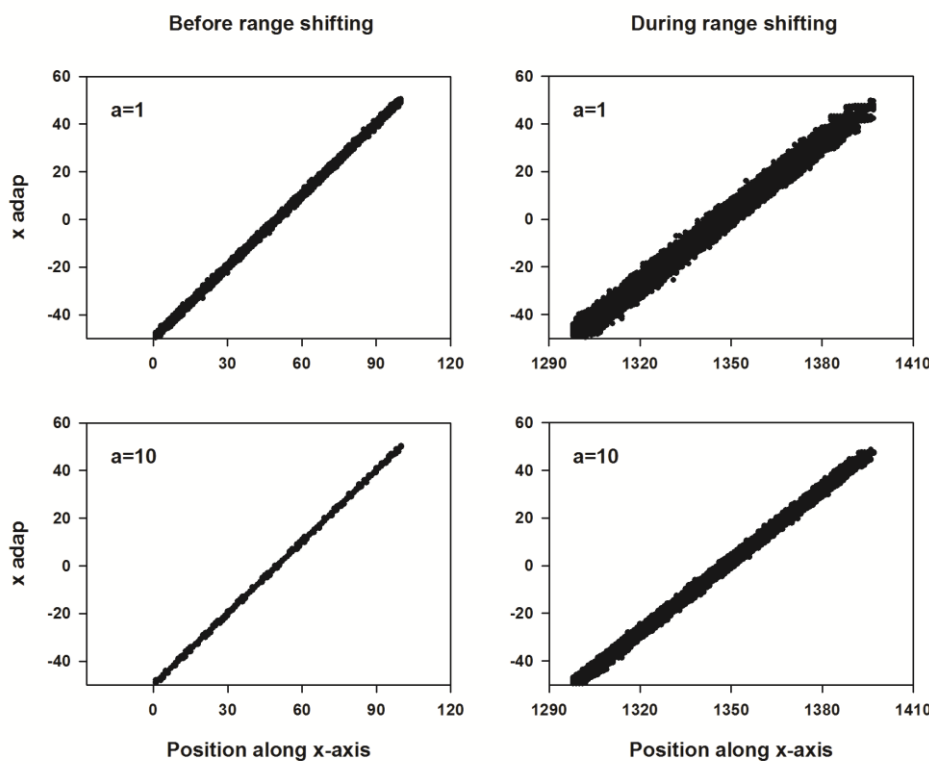


Figure S2.27: This figure represents the deviation in space (x_{adap}) along the x-axis of an individual's local optimum to the global optimum in function of position. This is done both before and during range shifting when evolution of x_{adap} is allowed. Each dot represents the genotype of a sampled individual. The global optimum of the population is located at the 50th column along the x-axis before range shifting and at the 1349th column during range shifting.

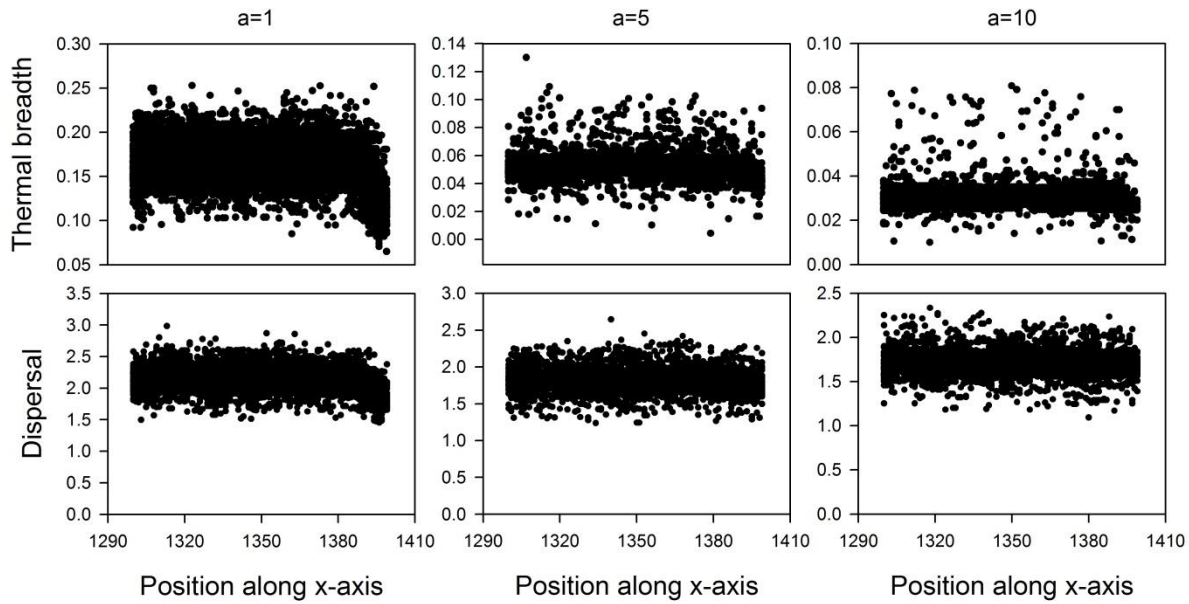


Figure S2.28: For several strengths of the performance-thermal breadth trade-off (α equaling 1, 5 or 10; equation 2), the resulting equilibrium in thermal breadth and dispersal during range shifting is displayed in function of position. One dot represents one sampled individual and the global optimum is positioned at the 1349th column along the x-axis. Here, the order of the competition-phase and the displacement-of-global-optimum phase in the lifecycle was switched.

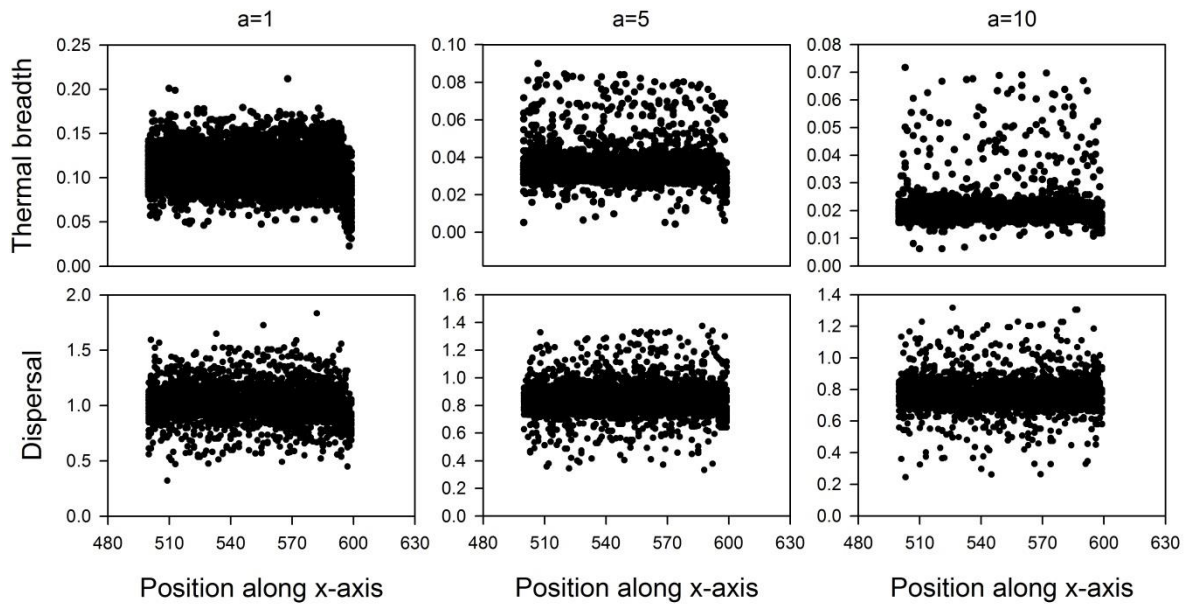


Figure S2.29: For several strengths of the performance-thermal breadth trade-off (α equaling 1, 5 or 10; equation 2), the resulting equilibrium in thermal breadth and dispersal during range shifting is displayed in function of position. One dot represents one sampled individual and the global optimum is positioned at the 549th column along the x-axis. The speed of range shifting was decreased to 0.5 columns per generation.

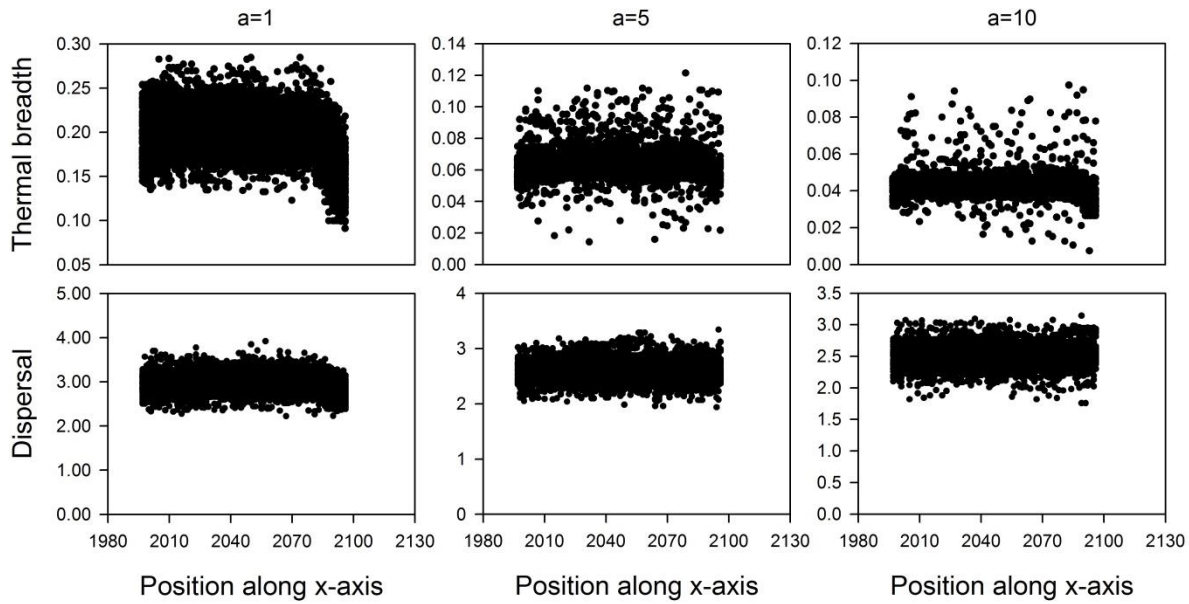


Figure S2.30: For several strengths of the performance-thermal breadth trade-off (α equaling 1, 5 or 10; equation 2), the resulting equilibrium in thermal breadth and dispersal during range shifting is displayed in function of position. One dot represents one sampled individual and the global optimum is positioned at the 2049th column along the x-axis. The speed of range shifting was increased to 2 columns per generation. For this scenario, the dimensions of the landscape were increased to 2110×100 .

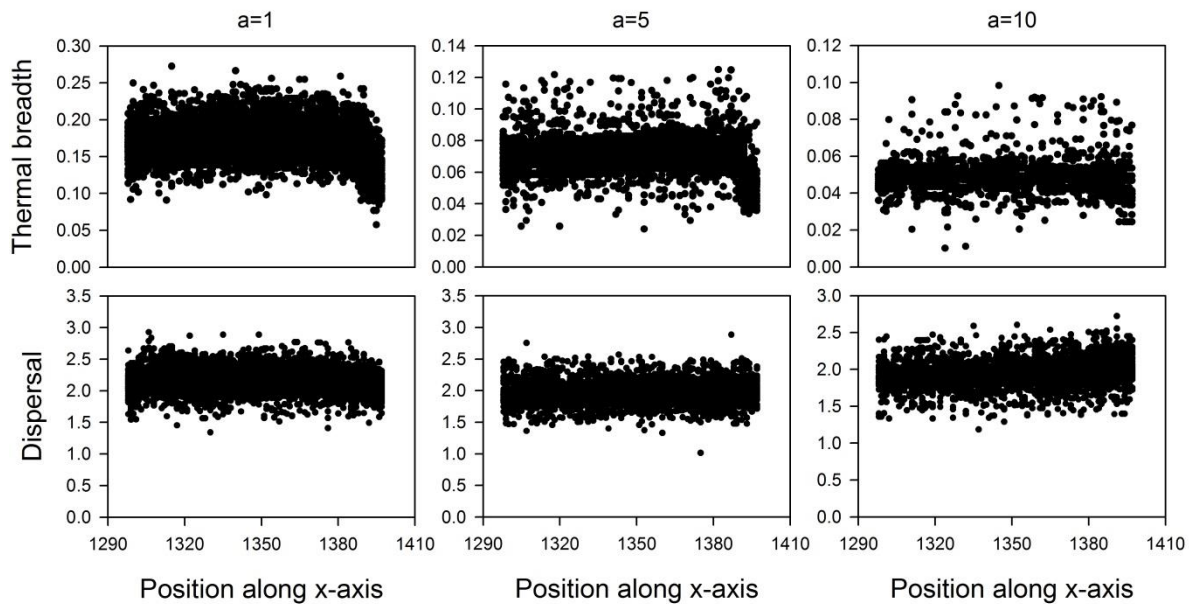


Figure S2.31: For several strengths of the performance-thermal breadth trade-off (α equaling 1, 5 or 10; equation 2), the resulting equilibrium in thermal breadth and dispersal during range shifting is displayed in function of position. One dot represents one sampled individual and the global optimum is positioned at the 1349th column along the x-axis. λ was decreased to 2.

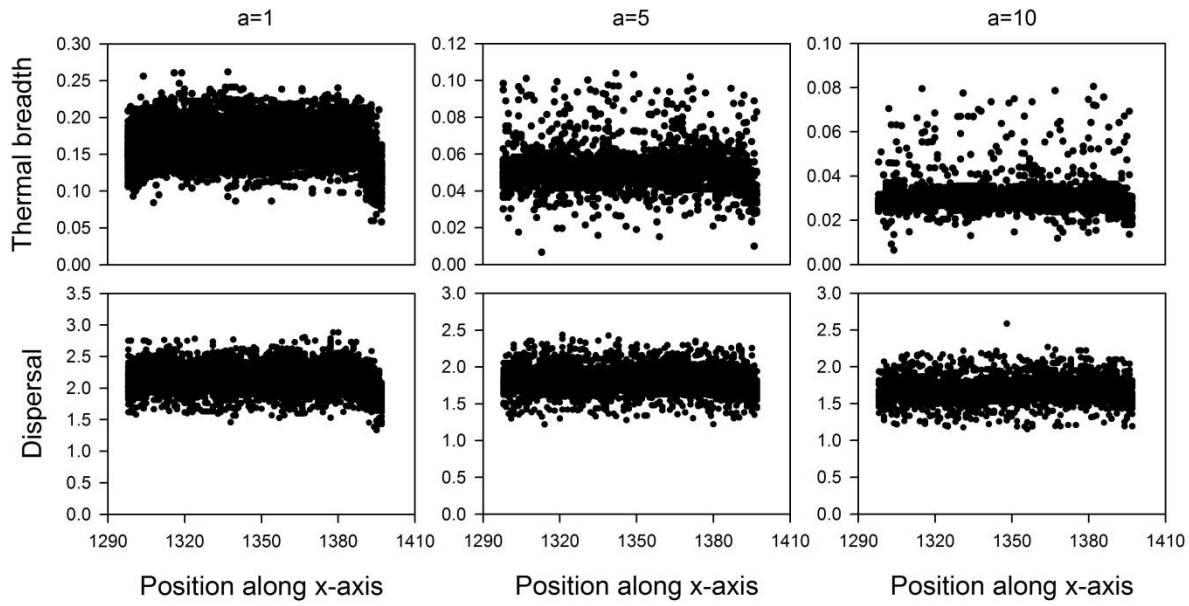


Figure S2.32: For several strengths of the performance-thermal breadth trade-off (α equaling 1, 5 or 10; equation 2), the resulting equilibrium in thermal breadth and dispersal during range shifting is displayed in function of position. One dot represents one sampled individual and the global optimum is positioned at the 1349th column along the x-axis. λ was increased to 5.

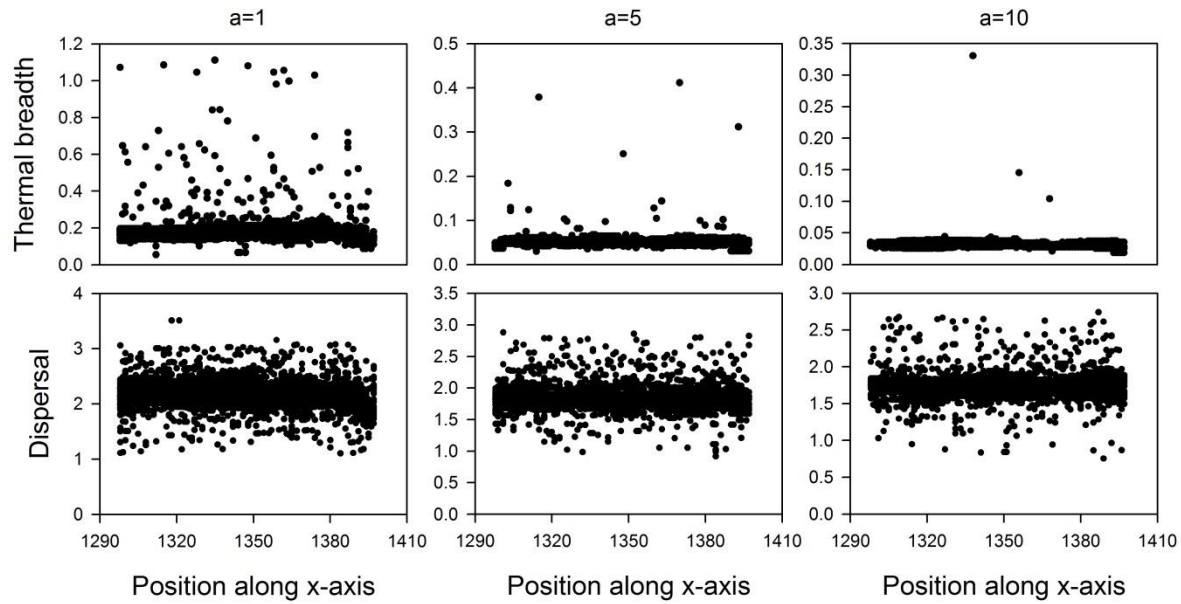


Figure S2.33: For several strengths of the performance-thermal breadth trade-off (α equaling 1, 5 or 10; equation 2), the resulting equilibrium in thermal breadth and dispersal during range shifting is displayed in function of position. One dot represents one sampled individual and the global optimum is positioned at the 1349th column along the x-axis. The mutationsizes of both dispersal and thermal breadth were increased to 1.

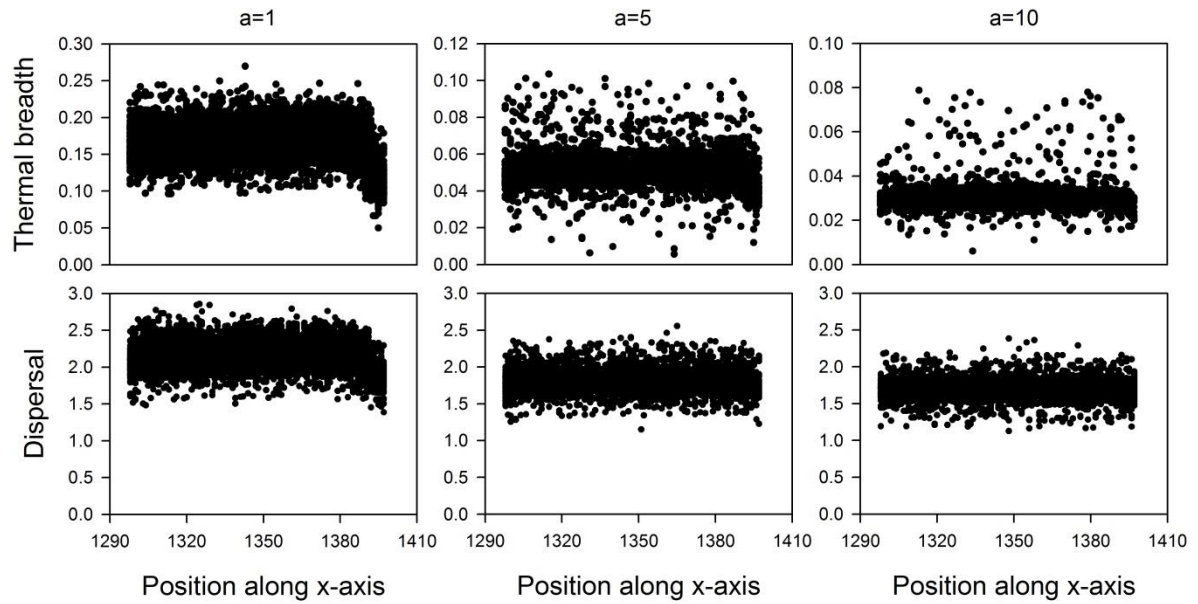


Figure S2.34: For several strengths of the performance-thermal breadth trade-off (α equaling 1, 5 or 10; equation 2), the resulting equilibrium in thermal breadth and dispersal during range shifting is displayed in function of position. One dot represents one sampled individual and the global optimum is positioned at the 1349th column along the x-axis. N^* was increased to 100.

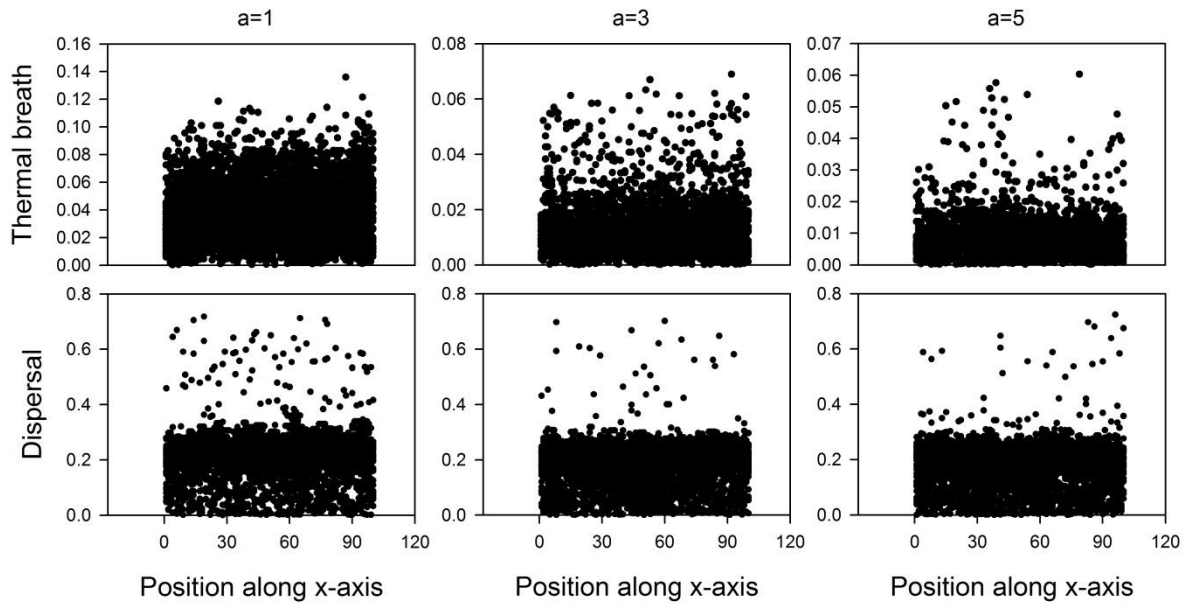


Figure S2.35: For several strengths of the performance-thermal breadth trade-off (a equaling 1, 3 or 5; equation 3), the resulting equilibrium in thermal breadth and dispersal before the start of range shifting is displayed in function of position. One dot represents one sampled individual and the global optimum is positioned at the 1349th column along the x-axis. The values of all parameters correspond to those used in the final figures (see Table 1).

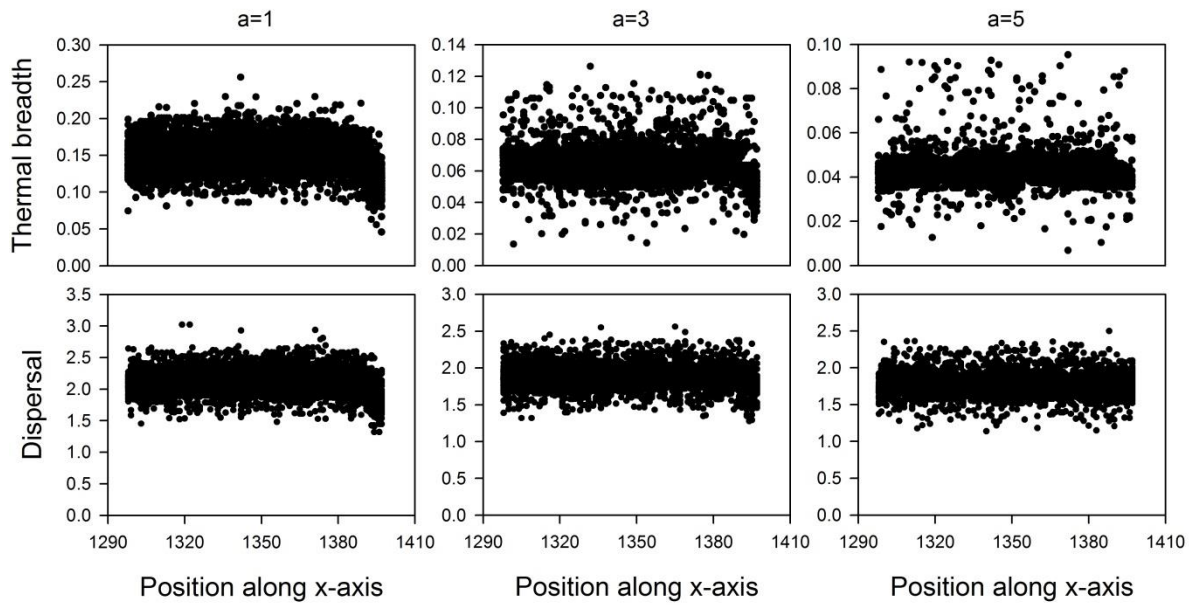


Figure S2.36: For several strengths of the performance-thermal breadth trade-off (a equaling 1, 3 or 5; equation 3), the resulting equilibrium in thermal breadth and dispersal during range shifting is displayed in function of position. One dot represents one sampled individual and the global optimum is positioned at the 1349th column along the x-axis. The values of all parameters correspond to those used in the final figures (see Table 1).

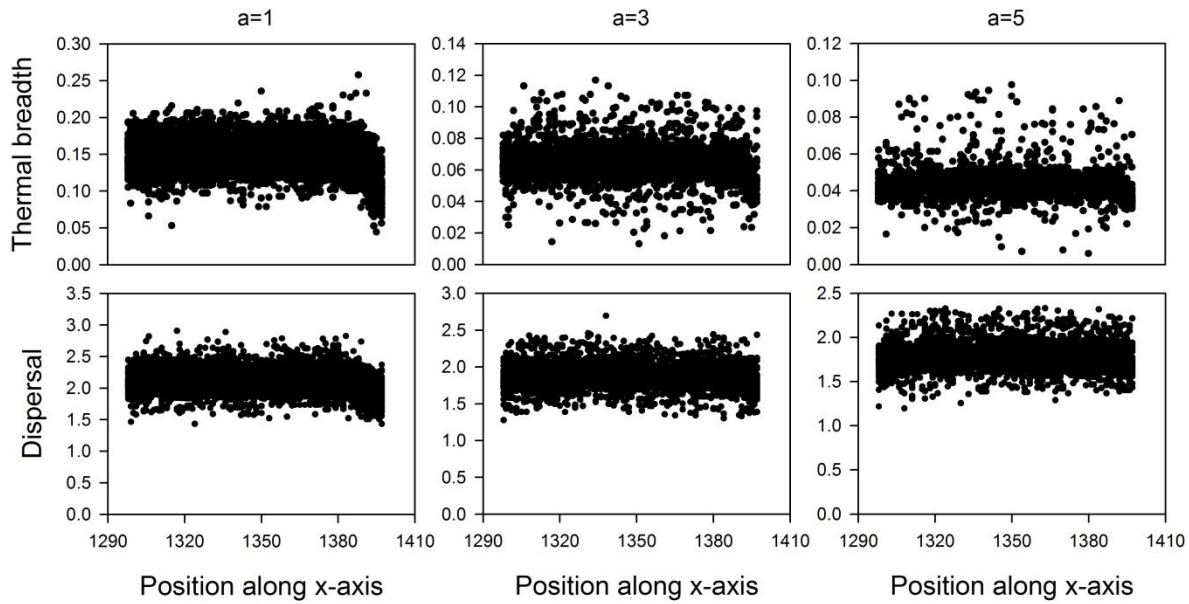


Figure S2.37: For several strengths of the performance-thermal breadth trade-off (α equaling 1, 3 or 5; equation 3), the resulting equilibrium in thermal breadth and dispersal during range shifting is displayed in function of position. One dot represents one sampled individual and the global optimum is positioned at the 1349th column along the x-axis. Here, the order of the competition-phase and the displacement-of-global-optimum phase in the lifecycle was switched.

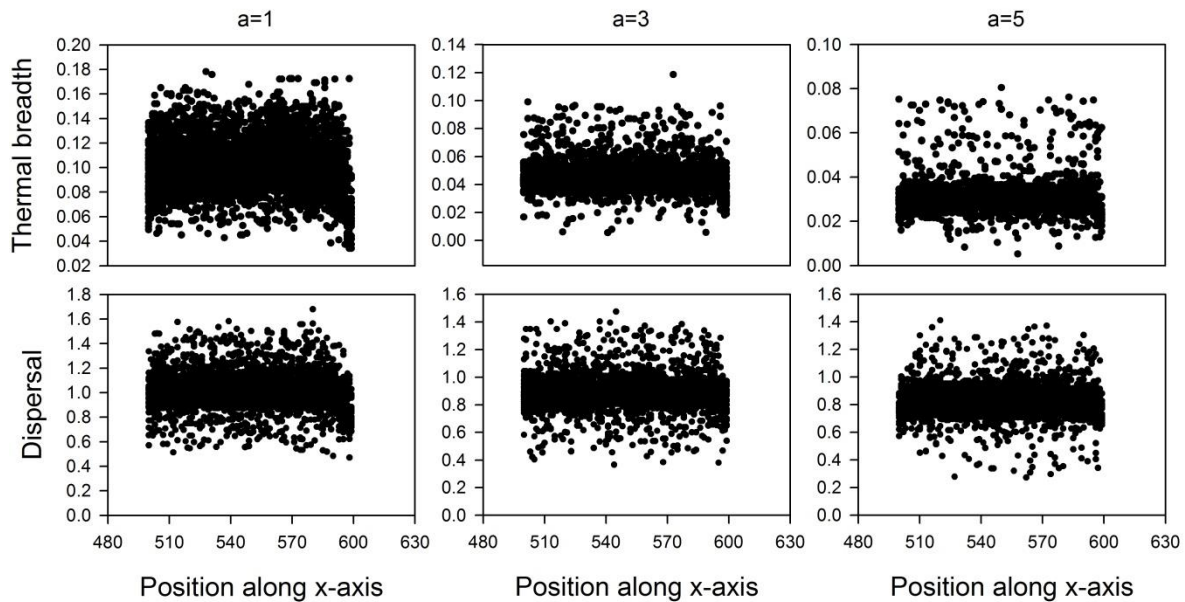


Figure S2.38: For several strengths of the performance-thermal breadth trade-off (α equaling 1, 3 or 5; equation 3), the resulting equilibrium in thermal breadth and dispersal during range shifting is displayed in function of position. One dot represents one sampled individual and the global optimum is positioned at the 549th column along the x-axis. The speed of range shifting was decreased to 0.5 columns per generation.

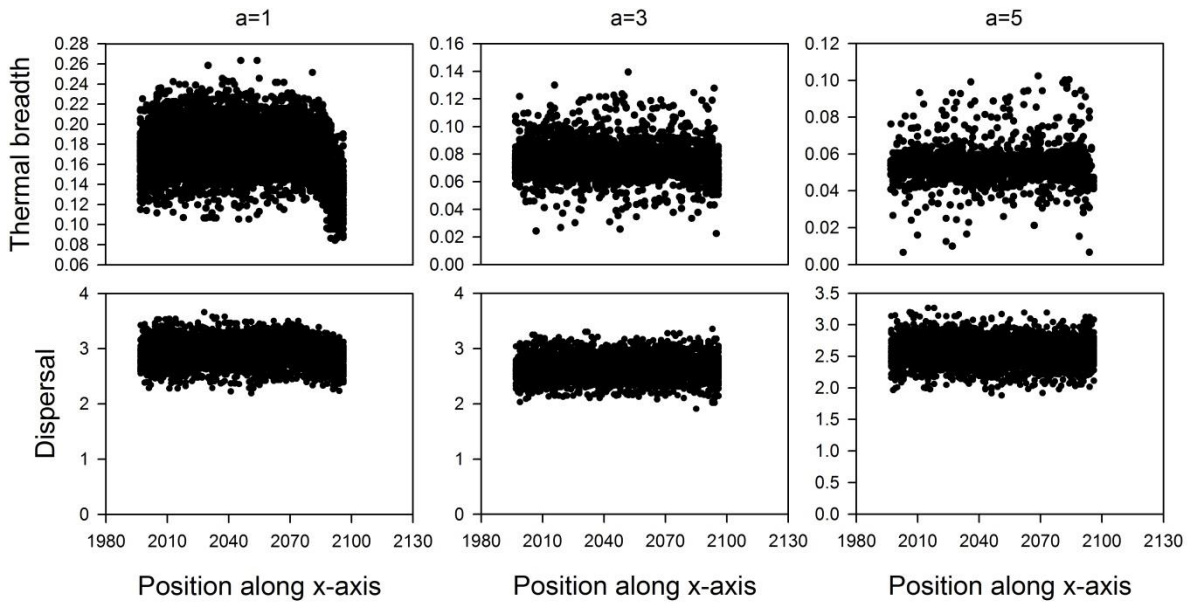


Figure S2.39: For several strengths of the performance-thermal breadth trade-off (α equaling 1, 3 or 5; equation 3), the resulting equilibrium in thermal breadth and dispersal during range shifting is displayed in function of position. One dot represents one sampled individual and the global optimum is positioned at the 2049th column along the x-axis. The speed of range shifting was increased to 2 columns per generation. For this scenario, the dimensions of the landscape were increased to 2110×100 .

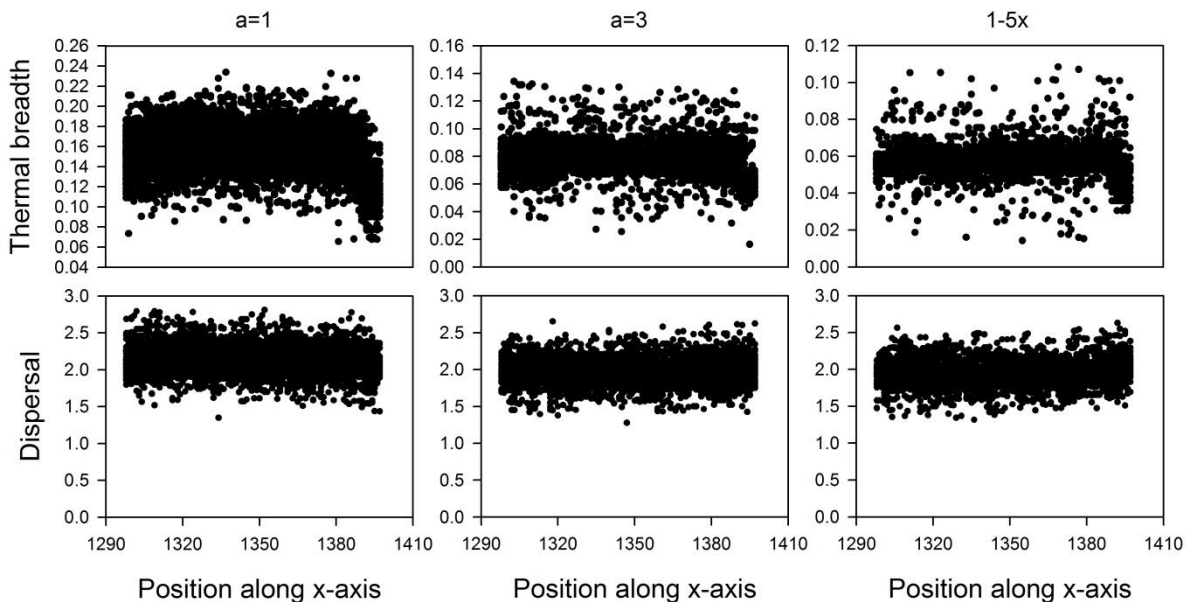


Figure S2.40: For several strengths of the performance-thermal breadth trade-off (α equaling 1, 3 or 5; equation 3), the resulting equilibrium in thermal breadth and dispersal during range shifting is displayed in function of position. One dot represents one sampled individual and the global optimum is positioned at the 1349th column along the x-axis. λ was decreased to 2.

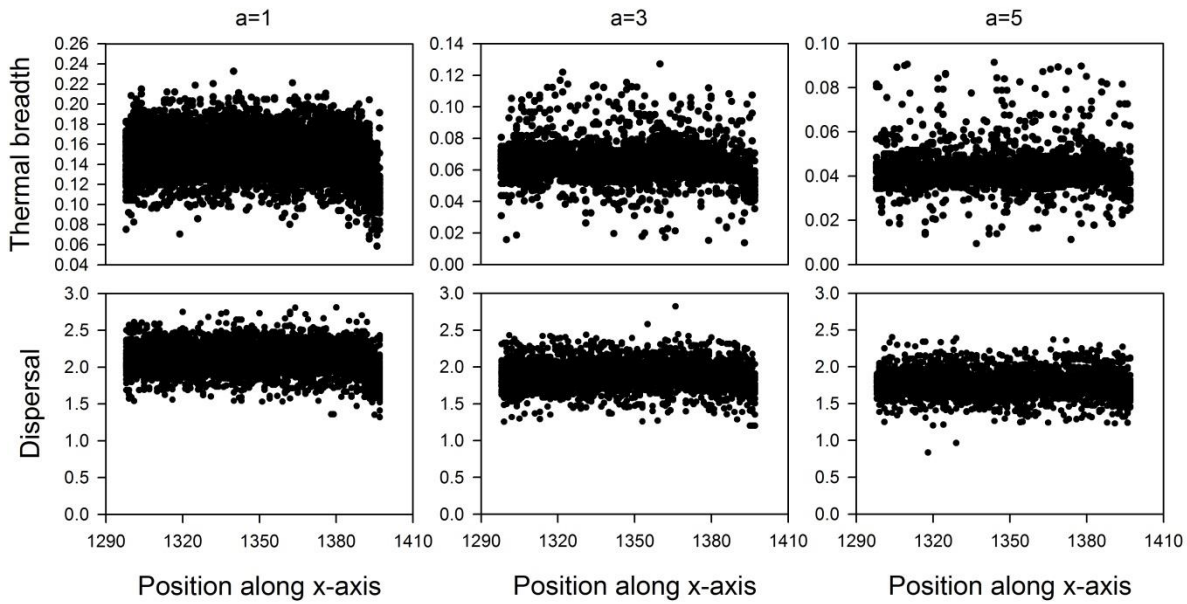


Figure S2.41: For several strengths of the performance-thermal breadth trade-off (α equaling 1, 3 or 5; equation 3), the resulting equilibrium in thermal breadth and dispersal during range shifting is displayed in function of position. One dot represents one sampled individual and the global optimum is positioned at the 1349th column along the x-axis. λ was increased to 5.

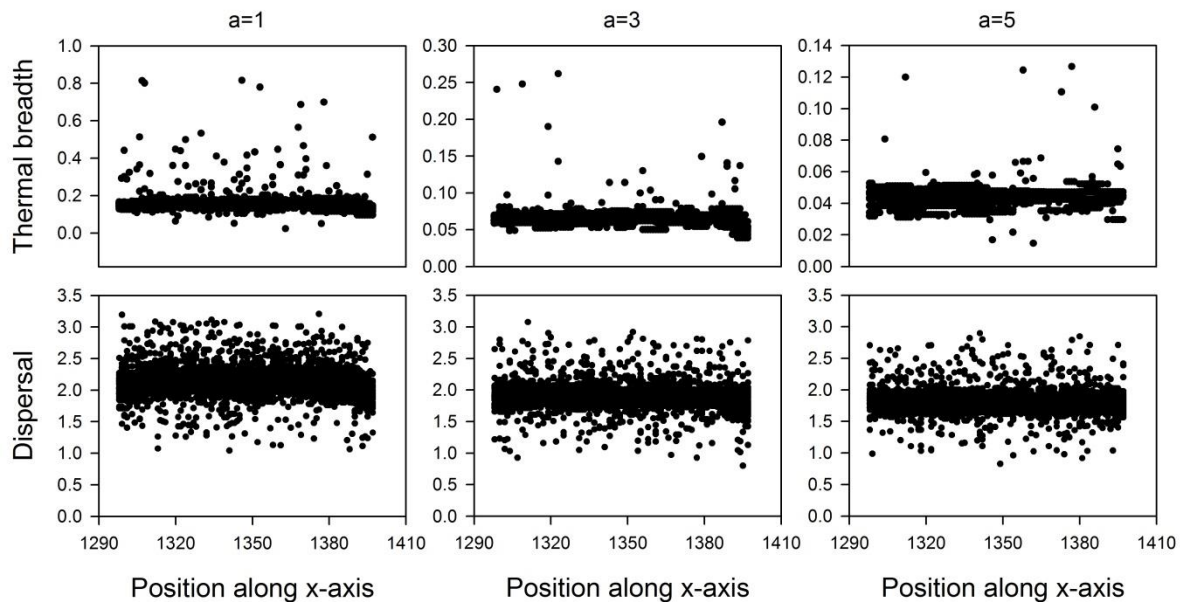


Figure S2.42: For several strengths of the performance-thermal breadth trade-off (α equaling 1, 3 or 5; equation 3), the resulting equilibrium in thermal breadth and dispersal during range shifting is displayed in function of position. One dot represents one sampled individual and the global optimum is positioned at the 1349th column along the x-axis. The mutationsizes of both dispersal and thermal breadth were increased to 1.

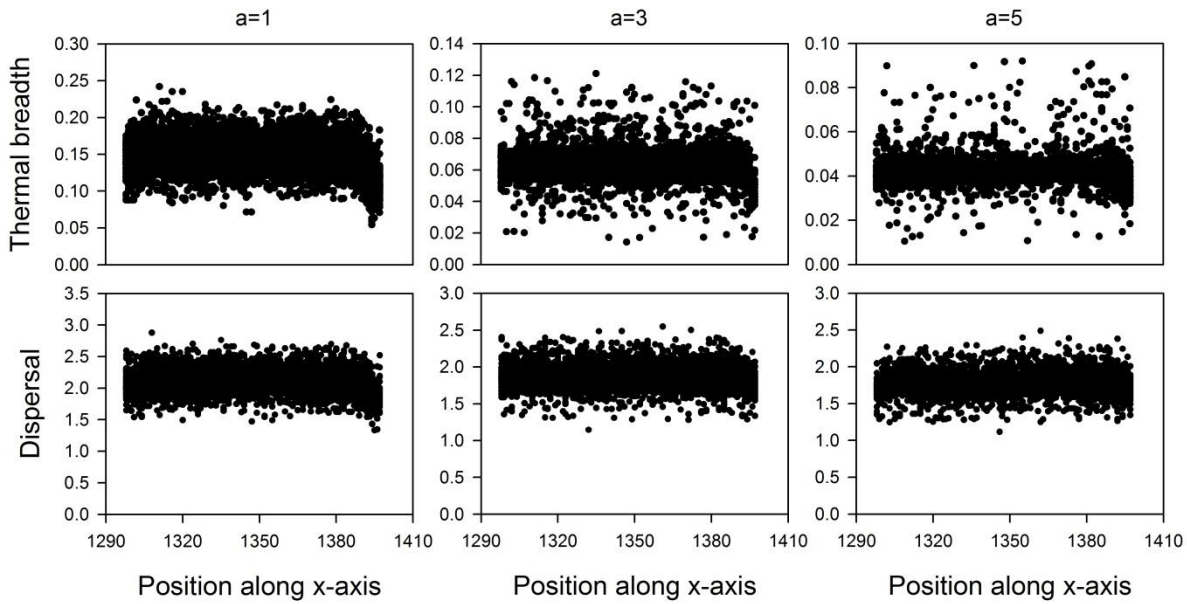


Figure S2.43: For several strengths of the performance-thermal breadth trade-off (α equaling 1, 3 or 5; equation 3), the resulting equilibrium in thermal breadth and dispersal during range shifting is displayed in function of position. One dot represents one sampled individual and the global optimum is positioned at the 1349th column along the x-axis. N^* was increased to 100.

When eq. (1) is used (Figures S2.44-S2.52) both traits are uniformly distributed within the range. Still, a small tendency toward individuals at the front having a narrower thermal breadth is observed. This is most clear when the speed of range shifting (cws) is high (Fig S2.48) or the mean number of descendants per individual (λ) is low (2) (Fig S2.49). Further, none of these discussed results differed qualitatively among all implemented trade-off functions.

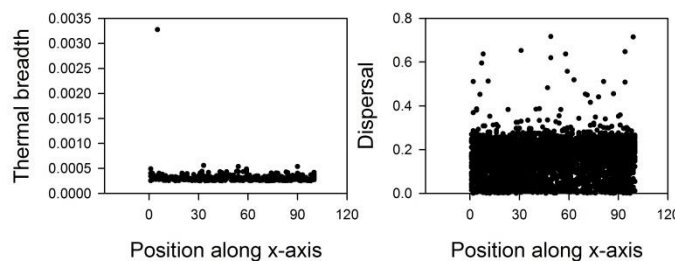


Figure S2.44: The equilibrium in thermal breadth and dispersal before the start of range shifting for equation 1 is displayed in function of position. One dot represents one sampled individual and the global optimum is positioned at the 1349th column along the x-axis. The values of all parameters correspond to those used in the final figures (see Table 1).

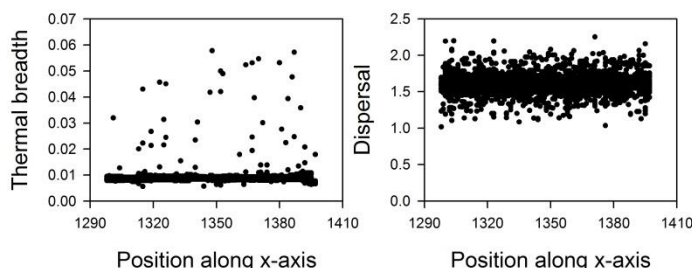


Figure S2.45: The equilibrium in thermal breadth and dispersal during range shifting for equation 1 is displayed in function of position. One dot represents one sampled individual and the global optimum is positioned at the 1349th column along the x-axis. The values of all parameters correspond to those used in the final figures (see Table 1).

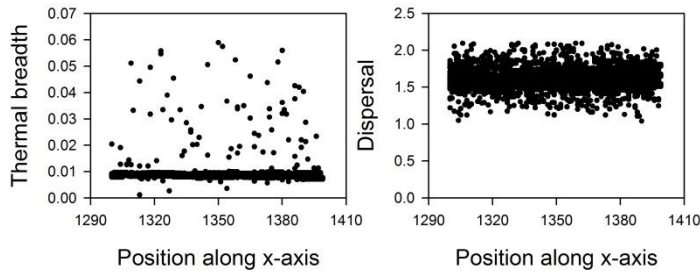


Figure S2.46: The equilibrium in thermal breadth and dispersal during range shifting for equation 1 is displayed in function of position. One dot represents one sampled individual and the global optimum is positioned at the 1349th column along the x-axis. Here, the order of the competition-phase and the displacement-of-global-optimum phase in the lifecycle was switched.

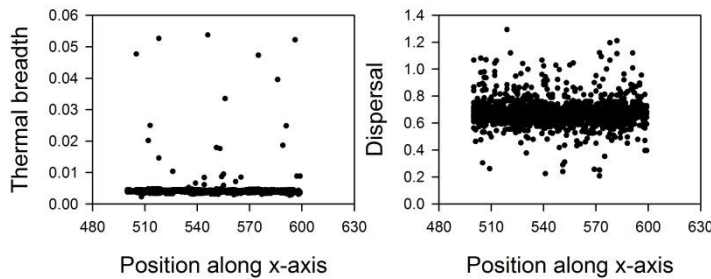


Figure S2.47: The equilibrium in thermal breadth and dispersal during range shifting for equation 1 is displayed in function of position. One dot represents one sampled individual and the global optimum is positioned at the 549th column along the x-axis. The speed of range shifting was decreased to 0.5 columns per generation.

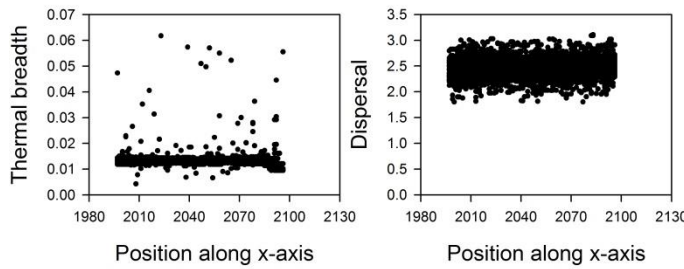


Figure S2.48: The equilibrium in thermal breadth and dispersal during range shifting for equation 1 is displayed in function of position. One dot represents one sampled individual and the global optimum is positioned at the 2049th column along the x-axis. The speed of range shifting was increased to 2 columns per generation. For this scenario, the dimensions of the landscape were increased to 2110 × 100.

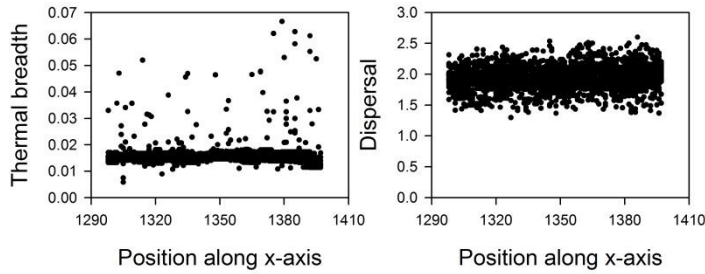


Figure S2.49: The equilibrium in thermal breadth and dispersal during range shifting for equation 1 is displayed in function of position. One dot represents one sampled individual and the global optimum is positioned at the 1349th column along the x-axis. λ was decreased to 2.

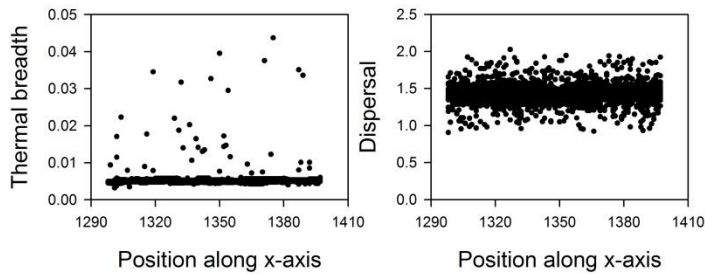


Figure S2.50: The equilibrium in thermal breadth and dispersal during range shifting for equation 1 is displayed in function of position. One dot represents one sampled individual and the global optimum is positioned at the 1349th column along the x-axis. λ was increased to 5.

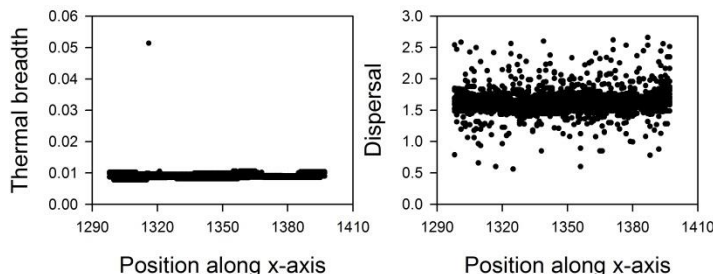


Figure S2.51: The equilibrium in thermal breadth and dispersal during range shifting for equation 1 is displayed in function of position. One dot represents one sampled individual and the global optimum is positioned at the 1349th column along the x-axis. The mutation sizes of both dispersal and thermal breadth were increased to 1.

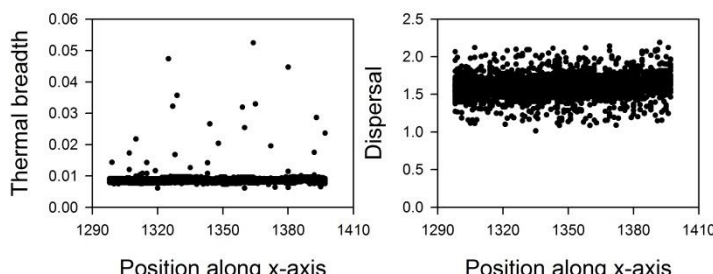


Figure S2.52: The equilibrium in thermal breadth and dispersal during range shifting for equation 1 is displayed in function of position. One dot represents one sampled individual and the global optimum is positioned at the 1349th column along the x-axis. N^* was increased to 100.